

5-31-2024

Methodology for developing biodegradable polymer blends and composites for agriculture

Fangzhong Xing

New Jersey Institute of Technology, xingfangzhongpersonal@gmail.com

Follow this and additional works at: <https://digitalcommons.njit.edu/theses>



Part of the [Materials Science and Engineering Commons](#)

Recommended Citation

Xing, Fangzhong, "Methodology for developing biodegradable polymer blends and composites for agriculture" (2024). *Theses*. 2593.

<https://digitalcommons.njit.edu/theses/2593>

This Thesis is brought to you for free and open access by the Electronic Theses and Dissertations at Digital Commons @ NJIT. It has been accepted for inclusion in Theses by an authorized administrator of Digital Commons @ NJIT. For more information, please contact digitalcommons@njit.edu.

Copyright Warning & Restrictions

The copyright law of the United States (Title 17, United States Code) governs the making of photocopies or other reproductions of copyrighted material.

Under certain conditions specified in the law, libraries and archives are authorized to furnish a photocopy or other reproduction. One of these specified conditions is that the photocopy or reproduction is not to be “used for any purpose other than private study, scholarship, or research.” If a user makes a request for, or later uses, a photocopy or reproduction for purposes in excess of “fair use” that user may be liable for copyright infringement,

This institution reserves the right to refuse to accept a copying order if, in its judgment, fulfillment of the order would involve violation of copyright law.

Please Note: The author retains the copyright while the New Jersey Institute of Technology reserves the right to distribute this thesis or dissertation

Printing note: If you do not wish to print this page, then select “Pages from: first page # to: last page #” on the print dialog screen

The Van Houten library has removed some of the personal information and all signatures from the approval page and biographical sketches of theses and dissertations in order to protect the identity of NJIT graduates and faculty.

ABSTRACT

METHODOLOGY FOR DEVELOPING BIODEGRADABLE POLYMER BLENDS AND COMPOSITES FOR AGRICULTURE

**by
Fangzhong Xing**

The use of polyethylene (PE) films to improve soil conditions and to increase crop yield has produced microplastics that are harmful to our ecosystem. The overall objective of this thesis is to develop an effective biodegradable polymer/composite to replace PE, and hence, to reduce microplastic pollution. The focus of this research is to develop a systematic protocol for assessing the suitability of the biodegradable films based on industry standards in agriculture. For this purpose, a range of biodegradable polymer blends are prepared using polylactic acid (PLA) and polybutylene adipate-co-terephthalate (PBAT) with varying PLA to PBAT ratios. Solvent casting combined with hot melt press procedure is developed for reproducible fabrication of films with controlled film thickness. The blend formulation is further tuned by incorporating nano-hydroxyapatite (n-HA) and microcrystalline cellulose (MCC) to enhance film properties. The effect of film composition on mechanical behavior, water absorption, thermal properties, and UV ageing is reported.

**METHODOLOGY FOR DEVELOPING BIODEGRADABLE POLYMER BLENDS AND
COMPOSITES FOR AGRICULTURE**

**by
Fangzhong Xing**

**A Thesis
Submitted to the Faculty of
New Jersey Institute of Technology
in Partial Fulfillment of the Requirements for the Degree of
Master of Science in Materials Engineering**

Department of Chemical and Materials Engineering

May 2024

APPROVAL PAGE

**METHODOLOGY FOR DEVELOPING BIODEGRADABLE POLYMER BLENDS
AND COMPOSITES FOR AGRICULTURE**

Fangzhong Xing

Dr. Lisa Axe, Thesis Advisor Date
Professor and Chair, Chemical and Materials Engineering, NJIT

Dr. Murat Guvendiren, Thesis Co-Advisor Date
Associate Professor, Chemical and Materials Engineering, NJIT

Dr. Xiaobing Li, Committee Member Date
Chemist II of Polymer Processing Institute, NJIT

Dr. Osnat Gillor, Committee Member Date
Professor of Ben-Gurion University of the Negev, Israel

BIOGRAPHICAL SKETCH

Author: Fangzhong Xing

Degree: Master of Science

Date: May 2024

Date of Birth:

Place of Birth:

Undergraduate and Graduate Education:

- Master of Science in Materials Engineering,
New Jersey Institute of Technology, Newark, NJ, 2023
- Bachelor of Art in Chemistry, University of Vermont, Burlington, VT, 2021

Major: Material Science and Engineering

ACKNOWLEDGMENTS

I extend my deepest gratitude to my advisors, Dr. Lisa Axe and Dr. Murat Guvendiren, for their invaluable guidance and unwavering support throughout this journey. Their expertise and insights have been pivotal in shaping both the direction and success of my work. Their patience and mentorship have not only guided this research but also influenced my growth as a scholar. During study preparation part, Dr. Li and Dr. Gillor gave me a lot of suggestions and thought.

I am grateful to the Biomedical Engineering department for providing access to the tensile machine, and the Polymer Processing Institute for the use of the hot press machine. The facilities and resources offered by these departments were crucial in the experimental phases of my research, enabling me to explore and validate my findings with state-of-the-art equipment.

I would like to acknowledge the generosity of NJIT-BGU Seed funding for the financial support.

Special thanks are due to my peer, Nikki C. Rodriguez, whose keen eye, and honest feedback were invaluable. Nikki's guidance in identifying presentation issues, assisting in finding the necessary machines, and advising on the ratio of blends contributed significantly to the refinement of my work.

TABLE OF CONTENTS

Chapter		Page
1	INTRODUCTION.....	1
2	LITERATURE REVIEW.....	6
2.1	Biodegradable Polymer Blends.....	6
2.2	Requirement Of Standard of BDM.....	18
2.3	Antibiotic Adsorption.....	20
3	HYPOTHESES AND OBJECTIVES.....	24
4	METHODS.....	25
4.1	Experiment Procedure.....	26
4.1.1	Solvent Casting.....	26
4.2	Thermogravimetric Analysis (TGA).....	28
4.3	Differential Scanning Calorimetry (DSC).....	28
4.4	Tensile Test.....	29
4.5	Water Absorption Test.....	29
4.6	UV Aging.....	30
4.7	Microplastic Preparation.....	31
4.8	Antibiotic Adsorption.....	31
5	RESULTS AND DISCUSSION.....	35
5.1	Sample Preparation.....	35
5.2	Mechanical Test.....	40

**TABLE OF CONTENTS
(Continued)**

Chapter		Page
	5.2.1 Pure Samples.....	42
	5.2.2 PBAT/PLA Blends.....	45
	5.2.3 PBAT/PLA Composite.....	49
5.3	Thermal Test.....	54
	5.3.1 Thermogravimetric Analysis (TGA).....	54
	5.3.2 Differential Scanning Calorimetry (DSC).....	58
5.4	Water Absorption.....	60
5.5	UV Aging.....	62
6	CONCLUSION AND FUTURE WORK.....	65
	REFERENCES.....	70

LIST OF TABLES

Table		Page
2.1	Mechanical Properties.....	9
2.2	Standard Of BDM Film Mechanical Properties Requirement EN 17033.....	11
4.1	Solvent Casting And Hot-Pressed Blend Samples wt% ...	26
4.2	Solvent Casting Composite Samples wt%.....	27
4.3	Concentrations To Be Used In The Study	33
5.1	Standards.....	39
5.2	Polymer Blends Found In Literature And EN17033 Requirement.....	41
5.3	Result Of Mechanical Test.....	43
5.4	Result Of Mechanical Test.....	47
5.5	Result Of Mechanical Test.....	52
5.6	Thermogravimetric Analysis For PBAT/PLA 90/10 Blend...	56
5.7	Thermal Parameters From 2nd Heating Scan Of Differential Scanning Calorimetry (DSC) Analysis.....	59

LIST OF FIGURES

Figure		Page
1.1	The amount of plastic sold in the EU for crop production and livestock in 2019.....	2
2.1	Chemical structure of PLA, PBAT, HA, and MCC.....	8
2.2	TG curves of composites with different proportions of n-HA addition.....	17
2.3	The mass changes of materials studied during the abiotic degradation testing at 70 °C.....	20
4.1	Experimental procedure.....	28
4.2	Antibiotic concentrations found in fresh water (FW) and treated wastewater (TWW) from Neve Ya'ar, Israel	33
5.1	A) solvent casted sample, dots are air bubbles, B) Hand-cut samples.	37
5.2	Hot melt pressed sample.....	40
5.3	Tensile stress result of composites with EN 17033 reference line.....	44
5.4	Tensile stress result of composites with EN 17033 reference line.....	44
5.5	Tensile stress result of composites with EN 17033 reference line.....	48
5.6	Tensile stress result of composites with EN 17033 reference line.....	48
5.7	Tensile strain vs tensile stress plot by sample 3 and sample 9.....	49
5.8	Tensile stress result of composites with EN 17033 reference line.....	52

**LIST OF FIGURES
(Continued)**

Figure		Page
5.9	Tensile strain results of composites.....	53
5.10	Stress vs Strain plot of Samples 13 to 18.....	53
5.11	A) TG curve of PLA/PBAT 10/90 blend, B) Derivative of PLA/PBAT 10/90 blend.....	57
5.12	DSC result of PBAT/ PLA 90/10 blend.....	60
5.13	Water absorption results of PLA majority samples.....	62
5.14	Mass loss during UV aging of PBAT/PLA composite.....	63

CHAPTER 1

INTRODUCTION

Recently, a major global concern is the increasing pollution of microplastics, also known as MPs. There is significant evidence of their impact on the water cycle, including agricultural systems (Kumar et al., 2020). The main sources of microplastic pollution in agricultural soils are the application of biosolids and composts, wastewater irrigation, polymer-based fertilizers and pesticides, atmospheric deposition, and mulch (Kumar et al., 2020). As part of addressing the pervasive issue of microplastic pollution, this research seeks to assess the potential of biodegradable polymer alternatives to mitigate its spread. Plastic films are being used more frequently due to their beneficial properties, which include increasing soil temperature, reducing weed pressure, retaining moisture, reducing pests, improving the efficiency of soil nutrients, and increasing crop yields (Amare et al., 2021). Polyethylene (PE) has been used extensively because of its mechanical properties. Although plastic films are effective in increasing crop yields, their impact and handling can lead to the emergence of microplastics in the environment. Only 9% of global plastics produced (Figure 1.1) are recycled, while

most are disposed in landfills, incinerated, and a large amount ends up as microplastics in the environment (Briassoulis, 2023).

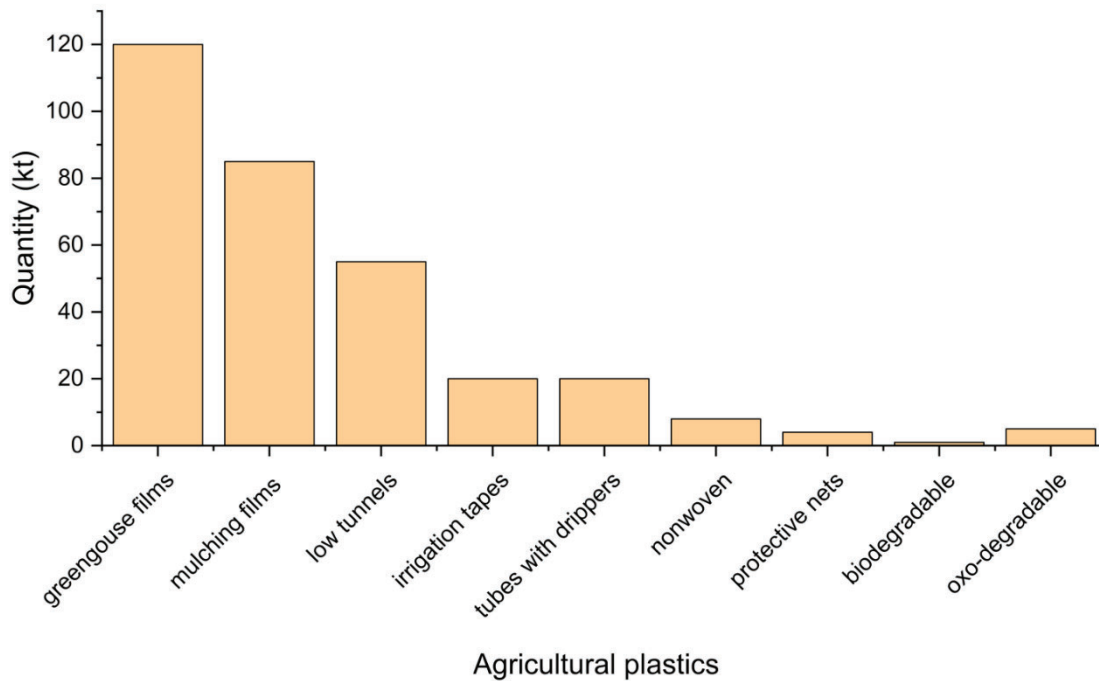


Figure 1.1 The amount of plastic sold in the EU for crop production and livestock in 2019 from Briassoulis (2023).

Source: Briassoulis, D. (2023). Agricultural plastics as a potential threat to food security, health, and environment through soil pollution by microplastics: Problem definition. *Science of the Total Environment*, 892, 164533. <https://doi.org/10.1016/j.scitotenv.2023.164533>

Vivo and vitro experiments have shown that microplastics can affect the digestive, respiratory, endocrine, reproductive, and the immune system (Lee et al., 2023).

Therefore, a biodegradable polymer blend or composite is needed to reduce the spread and impact of microplastics such as PE.

Past mulch contamination has led to the development of environmentally friendly alternatives, biodegradable mulch (BDM), with polymers such as polybutylene adipate-co-terephthalate (PBAT) and butylene succinate adipate (PBSA) (Jian et al., 2020; Kasirajan and Ngouajio, 2012). Theoretically, BDM decomposes and mineralizes over a period that does not impact the microbial community (Bandopadhyay et al., 2018). Zhou et al. (2022) demonstrated that the ester bond breakage and hydrolysis of polylactic acid (PLA) in soil formed water-soluble low molecular weight oligomers in degradation, which can be further degraded by bacteria. However, PLA's degradation rate is too slow as, for example, Ślęzak et al. (2023) reported only 1% mass loss after 12 months of degradation in soil. Nevertheless, PLA is a candidate for replacing traditional petroleum-based plastics. Advances in polymerization technology have significantly reduced production costs and helped make PLA economically competitive with petroleum-based polymers. PLA has other limitations that include low flexibility, low impact resistance, low thermal stability during processing, and low crystallinity; all of which will limit its application (Liu et al., 2011). Several researchers (Murariu et al., 2016, Nofar et al., 2015, Nofar et al., 2016) reported mechanical properties of blends of PBAT with PLA to optimize strain and flexibility. PBAT exhibits high strain, flexibility, and water resistance making it attractive in

polymer for blends in meeting requirements for agricultural application.

Researchers (Yin et al., 2019) have demonstrated that a PLA/PBAT blend can exhibit similar mechanical properties to PE.

Although BDM are innovative alternatives to traditional nondegradable plastic films, the surface may still have an affinity for not only contaminants such as antibiotics, but also for biofilms that may then promote antibiotic resistance genes (Arias-Andres et al., 2018). Applying hydroxyapatite is hypothesized to be a potentially viable addition for BDM in reducing the affinity of bacteria for the surfaces. Hydroxyapatite (HA) is a primary mineral component of bone and teeth and responsible for their hardness and strength. HA has been widely applied in medical, pharmaceutical, and chemical industries to help in bone repair (Sopyan et al., 2016) and in bioimplant coatings with its inherent properties such as thermal stability, ion-exchange capability, acid-base behavior, and relatively low antibacterial activity (Saxena et al., 2017). Yan et al. (2020) studied the properties of the PLA/PBAT blend modified by MCC and n-HA for bone tissue engineering material. For agriculture, HA would have the benefit of serving as a source of the nutrient phosphorus as well. In this research, microcrystalline cellulose (MCC) is introduced as a potential reinforcing material due to its physical and chemical properties (Yan et al., 2020). MCC has a low density, low cost, non-toxic, as well

as a high abundance of hydroxyl groups on the surface, which can increase water absorption and improve the biodegradation rate. One objective of this overall project is to study the BDM blend/composite for its affinity for antibiotics that may be present in treated wastewater (TWW) irrigation. It is expected that both contaminants and potential biofilms in the soil will have a reduced affinity for the BDM surfaces.

This research addresses establishing a methodology to achieve uniform and reproducible films for agriculture that have comparable properties to that of PE. The thesis includes a literature review on the selection of polymers and additives, objectives and hypotheses, methods to test the hypotheses, results, and conclusions and future work.

CHAPTER 2

LITERATURE REVIEW

This section reviews the challenges posed by microplastics and the role of biodegradable polymer blends, specifically PLA/PBAT, in addressing these challenges. It covers the production, properties, and potential applications of these materials in agriculture, focusing on their mechanical properties, biodegradability, and antibiotic adsorption capacity.

2.1 Biodegradable Polymer Blends

Plastic particles with a diameter of less than 1 micron are called microplastics, and due to the widespread use of plastics in today's world, more and more plastic particles are entering the environment. Li et al. (2023) summarized the impact of microplastics on human health. Humans can be exposed to microplastics through many routes, such as inhalation and food. Current studies on the toxicity of microplastics suggest that exposure to microplastics may cause intestinal damage, imbalance of microflora, metabolic disorders, and other diseases (Li et al., 2023). In this literature review, the environmental challenges posed by microplastics, and the promising solutions offered by biodegradable polymer blends, PLA/PBAT, are presented. This includes a detailed examination of the properties, production, and potential applications of these materials in agricultural settings, emphasizing their role in mitigating the

environmental impact of traditional plastic films. Key research findings on the mechanical properties, biodegradability, and the ability of these blends to adsorb antibiotics are highlighted, indicating their significance in addressing broader environmental and public health concerns related to plastic pollution and antibiotic resistance. Li et al. (2023)'s review also points out the need for further research to optimize these materials for practical use, ensuring they meet industry standards while being economically viable for widespread adoption.

For this research, one of the most promising biodegradable polymers is PBAT (Figure 2.1) because of its high rate of biodegradation (Jian et al., 2020). PBAT is produced through the poly-condensation of butanediol, adipic acid, and terephthalic acid, using polyester manufacturing technology (Jian et al., 2020). Jian et al. (2020) reported on a composability test of PBAT that showed a biodegradation rate of 80% in 100 days, and Witt et al. (2001) demonstrated that PBAT is easily compostable by microbial communities. The synthesis of PBAT involves three main phases: pre-mixing, pre-polymerization, and the final polymerization. During the preparation of PBAT, it is essential to maintain high vacuum conditions and temperatures exceeding 190°C. These conditions are necessary to promote condensation reactions and eliminate water as a byproduct. In the final polymerization phase, nucleating agents such as talc,

chalk, or silicon oxides can be employed to enhance the crystallization of PBAT.

PBAT's high biodegradability is attributed to the open carbon chain in its chemical structure, referred to as an aliphatic unit (Figure 2.1). This characteristic renders the polymer susceptible to hydrolytic degradation, allowing it to decompose in the presence of water.

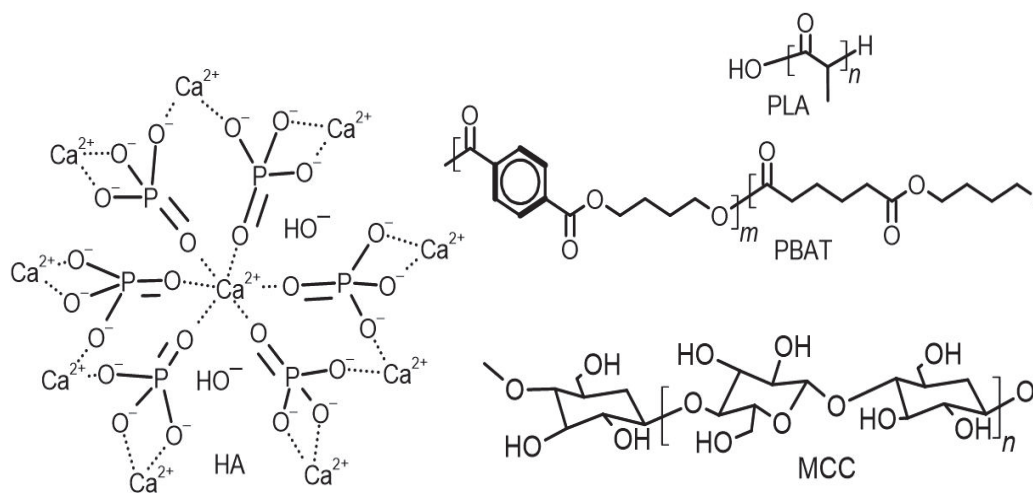


Figure 2.1 Chemical structure of PLA (from Mahapatro et al, 2011), PBAT (from Jian et al., 2020), HA (from Brunton et al. 2013), and MCC (from Liu et al., 2017).

Source: Mahapatro, A., & Singh, D. K. (2011). Biodegradable nanoparticles are excellent vehicle for site directed in-vivo delivery of drugs and vaccines. *Journal of Nanobiotechnology*, 9(1), 55. <https://doi.org/10.1186/1477-3155-9-55>

Jian, J., Xiangbin, Z., & Xianbo, H. (2020). An overview on synthesis, properties and applications of poly(butylene-adipate-co-terephthalate)–PBAT. *Advanced Industrial and Engineering Polymer Research*, 3(1), 19–26. <https://doi.org/10.1016/j.aiepr.2020.01.001>

Brunton, P., Davies, R. P. W., Burke, J., Smith, A. B., Aggeli, A., Brookes, S. J., & Kirkham, J. (2013). Treatment of early caries lesions using biomimetic self-assembling peptides – a clinical safety trial. *British Dental Journal*, 215(4), E6. <https://doi.org/10.1038/sj.bdj.2013.741>

Liu, W., Fei, M., Ban, Y., Jia, A., & Qiu, R. (2017). Preparation and Evaluation of Green Composites from Microcrystalline Cellulose and a Soybean-Oil Derivative. *Polymers*, 9(12), 541. <https://doi.org/10.3390/polym9100541>

The mechanical properties of PBAT demonstrate its high resistance to changes in shape, with an elongation break of 670%, which is greater than polyethylene, exhibiting a range of 1.2% to 12.9% (Table 2.1)

Table 2.1 Mechanical Properties

Property	Units	Polyethylene ¹	PBAT ²	PLA ³	MCC ⁴
Yield Strength	MPa	26.2 – 31	7.5	70	-
Tensile Stress	MPa	22.1 – 31	21	59	2.22 - 6.5
Elongation	% strain	11.2 – 12.9	670	7	-
Hardness	MPa	77.5 – 97.1	-	-	26 - 81
Impact Strength	kJ/m ²	1.90 – 200	-	-	-
Young's Modulus	MPa	1070 – 1090	126	1280	-

Sources:

¹Manufacturing, D., 2021. Polyethylene (HDPE/LDPE). <https://dielectricmfg.com/knowledge-base/polyethylene/>.

²Jian, J., Xiangbin, Z., Xianbo, H., 2020. An overview on synthesis, properties and applications of poly(butylene-adipate-co-terephthalate)–PBAT. *Advanced Industrial and Engineering Polymer Research* 3(1), 19-26. <https://doi.org/https://doi.org/10.1016/j.aiepr.2020.01.001>.

³Farah, S., Anderson, D. G., & Langer, R. (2016). Physical and mechanical properties of PLA, and their functions in widespread applications — A comprehensive review. *Advanced Drug Delivery Reviews*, 107, 367–392. <https://doi.org/10.1016/j.addr.2016.06.012>

⁴ Elsakhawy, M., Hassan, M., 2007. Physical and mechanical properties of microcrystalline cellulose prepared from agricultural residues. *Carbohydrate Polymers* 67(1), 1-10. <https://doi.org/10.1016/j.carbpol.2006.04.009>.

In contrast, PE is a stronger material with a higher tensile strength ranging from 22.1 to 31 MPa. Furthermore, at a consumer scale, PBAT is expensive to manufacture; a composite can potentially address the limitations of PBAT (Jiao

et al., 2020b). Inexpensive materials such as starch or reinforcing materials like PLA can be added. PLA's tensile strength of 59 MPa is greater than that of PBAT which is approximately 21 MPa (Table 2.1). PLA can reinforce PBAT in a blend due to its higher resistance to breaking under tension. Starch is a readily available compound made up of carbon, hydrogen, and oxygen, and it is biodegradable, belonging to the class of carbohydrate organic compounds including MCC. MCC is characterized by high toughness and low density, making it a great candidate as a reinforcement material. Furthermore, the hydroxyl groups present on MCC surfaces form hydrogen bonds with other materials to improve water adsorption and expedite biodegradability (Naseri et al., 2016). PLA is a biodegradable polymer that is relatively inexpensive to produce. Overall, a blend of PBAT and PLA may potentially exhibit properties that meet the European Standard EN 17033 (Table 2.2): tensile strength at break and elongation at break properties for developing a durable mulch film coating, while also supporting biodegradability.

Table 2.2 Standard of BDM film mechanical properties requirement EN 17033

	Thickness (μm)		
	≤ 10	$10 \leq X \leq 15$	$15 \leq$
Tensile stress – lengthwise (MPa)	16	18	18
Tensile stress – Crosswise (MPa)	16	16	16
Strain – lengthwise (%)	100	150	200
Strain – Crosswise (%)	250	300	350
Impact resistance (g)	60	80	100
Tolerance of average thickness (%)	10	10	10

In general, properties related to durability are crucial for the development of PBAT-based biodegradable films. Positive results have been achieved with PBAT/PLA/nanoparticle composites (agricultural films manufactured by KINGFA) in crop applications in China (Jian et al., 2020). They reported that the biodegradation rate of pure PBAT mulch showed 80% mass loss in 45 days and was observed to completely degrade over a period of 3 months in industry composting. National Geographic Society (NGS) (Bandyopadhyay et al., 2023) reported PE films accelerate crop harvest about 7 to 14 days in advance. However, Jian et al. (2020) reported that PBAT mulch did not perform sufficiently over the growth period of 90 days. Gao et al. (2021) reported that

the PBAT blend started degradation after approximately 60 days and then lost integrity after 120 days. Jian et al. (2020) reported that the properties of pure PBAT alone are not sufficient for application due to its higher production costs and lower mechanical properties compared to conventional plastics. The incorporation of low-cost materials like starch and reinforcing materials such as PLA is as an effective strategy to improve these properties while maintaining the biodegradability of the composites.

Fu et al. (2020) produced PBAT and PLA blends and tested their biodegradation rates in freshwater sediment and water collected from Hebei, China. The pure PLA and pure PBAT polymer films were observed to break in pieces much more rapidly than the PLA/PBAT blends. After 24 months, pure PBAT and pure PLA films became brittle and easily fragmented. For PLA-75/PBAT-25, PLA-50/PBAT-50 and PLA-25/PBAT-75, mulch remained after 24 months of immersion in water. However, several months of incubation in fresh water, changes in the appearance of the polymer films indicated degradation of both PBAT and PLA components. Films show signs of degradation such as discoloration, corrosion holes, brittleness, and the formation of internal defects and cavities. Furthermore, analysis of the chemical structure and aggregate structure of the degradation residues confirmed the degradation of PBAT and PLA components. The molecular weight of the PLA/PBAT blend decreased, while the concentration of C-O bonds in the composite increased, indicating

degradation of the sample. The biodegradation rates of PBAT and PLA in PLA/PBAT blends were lower than those of their respective pure polymer forms. PBAT/PLA blends do biodegrade, albeit at different rates compared to the individual polymers. This study highlights the advantages of adding reinforcements such as PLA to PBAT to increase the longevity of the mulch while still maintaining its biodegradability. Although PLA/PBAT blends can produce a durable and BDM film, BDMs are susceptible to biofilm growth. Biofilm growth on biodegradable plastics, such as polyester-based materials, is an important ecological process that helps reduce environmental plastic pollution as MPs produced can be quickly decomposed (Leow et al., 2021). Biofilms however have been found to support the dissemination of antibiotic resistance genes (ARGs). The proximity and long retention time of cells within the biofilm matrix facilitate the exchange and recycling of nucleic acids, including ARGs. Horizontal gene transfer (HGT) mechanisms such as conjugation, transformation, transduction, and outer membrane vesicle (OMV)-mediated transfer can occur within biofilms, leading to the transfer of ARGs between bacteria (Michaelis et al., 2023). To reduce bacterial attraction to the surface, hydroxyapatite, a nutrient-dissolving mineral, may be effective.

Applying hydroxyapatite is hypothesized to be a potentially viable additive for BDMs in reducing the affinity of bacteria for the surfaces (Sopyan et al., 2016). Hydroxyapatite (HA) ($\text{Ca}_{10}(\text{PO}_4)_6(\text{OH})_{2(s)}$) (Figure 2.1) is a primary

mineral component of bone and teeth and responsible for their hardness and strength. HA has been widely applied in medical, pharmaceutical, and chemical industries to help in bone repair (Sopyan et al., 2016) and in bioimplant coatings due to its properties that include thermal stability, ion-exchange capability, acid-base behavior, and relatively low biotic activity (Saxena et al., 2017). Yan et al. (2020) studied the properties of the PLA/PBAT blend modified with nanohydroxyapatite (n-HA) for bone tissue engineering material. They also used microcrystalline cellulose (MCC) as a reinforcing material due to its unique physical and chemical properties; its properties include hardness ranging from 26.2 – 81.1 MPa and a high abundance of hydroxyl groups on the surface (Figure 2.1). Hydroxyl groups will increase water absorption ability then lead faster degradation. Yan et al. (2020) formed the PLA/PBAT/MCC/n-HA composites through hot melt press and observed the thermal stability of the composite improved after adding n-HA. With the addition of 6% by wt of n-HA, the blend exhibited improved tensile strength and water absorption as well. These properties can be altered based on the concentration of n-HA. Although this research was focused on bone tissue engineering, results demonstrate the compatibility between PBAT, PLA, MCC, and n-HA and how their mechanical properties can be enhanced for film production.

With respect to agricultural applications, n-HA significantly affects soil quality, plant growth, and microbial communities. n-HA is considered an

alternative to phosphorus fertilizers. Jia et al. (2022) reported that the application of n-HA increased soil bioavailable phosphorus, electrical conductivity, and soil organic matter while maintaining soil pH. The application of n-HA did not change the biodiversity of the soil microbial community but increased the abundance of beneficial bacteria related to phosphorus solubilization. n-HA is more soluble under acidic conditions increasing its bioavailability. Although n-HA did not significantly change the overall diversity of soil microbial communities, it did induce changes in bacterial community structure. Jia et al. observed an increase in the abundance of rhizosphere bacteria associated with plant growth. This research suggests that n-HA may promote overall beneficial microbial communities for plant growth.

As an alternative to traditional films, Sintim et al. (2017) proposed the following criteria in demonstrating the viability of a biodegradable film: (1) maintain a microclimate conducive to plant growth, (2) be flexible to install into soil (3) remain intact during planting season, (4) completely degrade once mulched into the soil or through composting, (5) pose no adverse effects on the environment, and (6) be economical. Gao et al. (2021) applied the PLA/PBAT film in agriculture and found it was as effective as PE films. However, the impact of the MPs formed from harvesting crops was not investigated.

Abed et al. (2023) studied the antibacterial properties of films with n-HA. The films were tested against *Escherichia coli* and *Staphylococcus aureus*. The results showed that films exhibited antimicrobial effects against these microorganisms. Importantly, the incorporation of n-HA into the film significantly improved its bacterial resistance compared to pure films. HA nanoparticles bind with protein molecules, which inhibits cellular metabolism and leads to cell death (Baskar et al., 2017).

Yan et al. (2020) demonstrated that the addition of n-HA in the composite improved the thermal stability of the material. As n-HA increased in concentration, thermogravimetric (TG) analysis revealed an increased thermal degradation temperature by about 20°C. Essentially, the n-HA-free PLA/PBAT composites begin to degrade at around 300°C, while the addition of n-HA results in a degradation temperature even higher. When the temperature rises, the molecular chain with carboxyl terminals degrades first (Figure 2.2). After adding n-HA particles, a large number of hydroxyl groups on the surface interact with the terminal carboxyl groups, reducing the number of free carboxyl terminals. Both MCC and n-HA have hydroxyl groups on their surfaces that adsorb water. As the addition of n-HA increases hydroxyl groups increase and can form hydrogen bonds with water molecules. Bound water accelerates hydrolysis of the composite. The hydroxyl groups on the surface of n-HA and MCC further hydrolyze ester groups in PLA and PBAT, destroying the main

chain structure of the matrix material, reducing the molecular weight, and accelerating degradation.

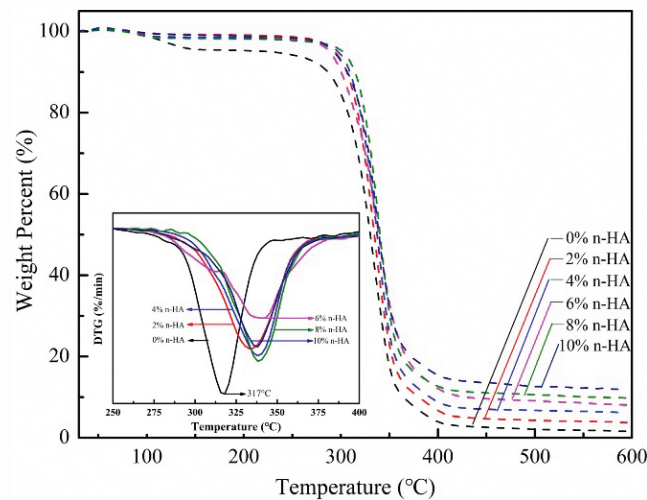


Figure 2.2 TG curves of composites with different proportions of n-HA addition from Yan et al., (2020).

Source: Yan, D., Wang, Z., Guo, Z., Ma, Y., Wang, C., Tan, H., & Zhang, Y. (2020). Study on the properties of PLA/PBAT composite modified by nanohydroxyapatite. *Journal of Materials Research and Technology*, 9(5), 11895–11904. <https://doi.org/10.1016/j.jmrt.2020.08.062>

Yin et al. (2019) investigated the impact of biodegradable film mulches (BDM) compared with conventional polyethylene (PE) mulches on crop growth and agricultural sustainability. This study compared BDM compounds with cornstarch, polycaprolactone, and a proprietary additive mixture without mulching. They analyzed the effects of these treatments on soil moisture, soil temperature, crop growth, and overall productivity during three growing seasons. BDM were found to support economic benefits. Growing with BDM can increase crop yields and generate greater net income compared to polyethylene mulch. Although the input cost of biodegradable films is greater,

labor costs are lower due to reduced labor requirements for handling residual films. It is important to note that the performance of BDMs may vary depending on environmental conditions, crop species, and field management systems. The film is used to retain soil moisture and increase the efficiency of irrigation water use. Research is needed in understanding the performance of biodegradable film mulches in increasing soil temperature, retaining moisture, and increasing crop yields. Therefore, further research is needed to improve the application and performance of BDM films. Overall, the use of BDMs in agriculture has the potential to provide similar benefits to polyethylene film mulching while also addressing the environmental concerns associated with plastic waste.

2.2 Requirement of Standard of BDM

All BDM must meet the EN 17033 standard, which includes tensile stress greater than 18 MPa, tensile strain greater than 200% lengthwise and 350% crosswise, and over 90% conversion to carbon dioxide within 2 years (Table 2.2). Fu et al. (2020) reported that blends with higher water absorption capacity show greater degradation rates. Weng et al. (2013) found that, upon mulching into soil after 4 months, both PLA and PBAT samples degraded faster than their blends, with PLA showing significant decomposition. This was evidenced by a decrease in organic carbon content and an increase in oxygen concentration in the residual samples, likely due to increased carboxyl groups.

Different conditions led to varying degradation rates in PLA/PBAT blends, with the fastest being a 50% mass loss within 70 days, as reported by Musioł et al. (2018) (Figure 2.3). During the study by Musioł et al. (2018), there was a systematic decrease in the mass of all samples during simulated industrial composting. This trend indicates that consistent degradation processes occur in all samples studied. There was a slight decrease in mass of the blend initially, followed by a more pronounced mass loss. This pattern is characteristic of hydrolytic degradation and indicates that the material is breaking down through hydrolysis. It is further demonstrated that adjusting the water absorption of the material can also control the degradation rate. This suggests that higher degradation rates will accelerate the decomposition of MP and that microplastics produced by using BDM will not persist permanently in the soil like MP produced by ordinary mulch films.

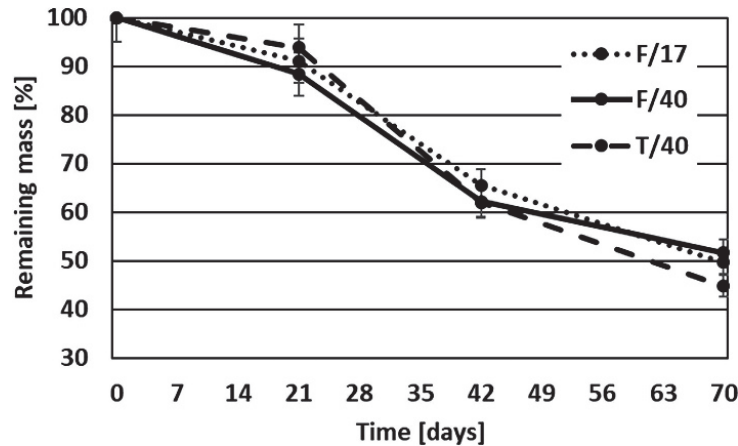


Figure 2.3 The mass changes of materials studied during the abiotic degradation testing at 70 °C from Musioł et al. (2018). F/17: 83/17 PBAT/PLA; F/40: 60/40 PBAT/PLA; and T/40: 60/40 PBAT/PLA.

Source: Musioł, M., Sikorska, W., Janeczek, H., Wałach, W., Hercog, A., Johnston, B., & Rydz, J. (2018). (Bio)degradable polymeric materials for a sustainable future – part 1. Organic recycling of PLA/PBAT blends in the form of prototype packages with long shelf-life. *Waste Management*, 77, 447–454. <https://doi.org/10.1016/j.wasman.2018.04.030>

2.3 Antibiotic Adsorption

Numerous antibiotics have been detected in both treated wastewater and freshwater sources. When animals are treated with antibiotics, not all the drugs are absorbed by their bodies. It is estimated that between 10 and 70% is excreted from the body and can enter the soil through the manure (Zheng et al., 2018). The introduction of antibiotics into the soil creates environmental stresses that lead to the evolution of certain microbial protective mechanisms (Zhang et al., 2021). These mechanisms include mutations in the genetic material of the nucleus, which ultimately lead to the production of antibiotic genes (ARG) (Zhang et al., 2021). These genes can then be replicated or transmitted through vertical and horizontal gene transfer between different

microbial populations, allowing them to persist in the soil for long periods of time (Zhang et al., 2022). Antibiotic resistance has emerged as a severe global public health concern, with ARGs originating from diverse sources, including soil, fertilizers, irrigation water, and the atmosphere (Deng et al., 2022).

Therefore, assessing the antibiotic adsorption capacity of mulches has become a crucial factor. If microorganisms carry multidrug ARGs, bacteria may develop resistance to multiple antibiotics, potentially evolving into superbugs, which are a significant threat to human health. Deng et al. (2022) reported that the soil-air-phylosphere pathway contributes the most to the accumulation of ARGs in the lettuce leafosphere and can be effectively blocked by covering the crop. The abundance of ARGs in the phyllosphere is then significantly reduced, resulting in reduced ARG uptake by humans through the food chain. However, Seyoum et al. (2021) reported that soil covered with film can exhibit an increased concentration of ofloxacin, highlighting the need for the development and study of mulches that do not adsorb antibiotics.

The literature review examined the challenges posed by microplastics and the properties of biodegradable polymer blends. In this chapter, current research was reviewed into the use of PLA/PBAT blends in agricultural applications and highlights the need for further development of higher strength films to ensure these materials are both effective and economically viable.

Additionally, this review demonstrated that while a standard exists for BDM films used in agriculture, there is not a systematic set of analyses used by researchers to develop novel blends and composites.

In the next chapter, hypotheses and objectives are presented and followed by the methodology. The subsequent methods section of this paper will focus primarily on the production process of BDM using PLA/PBAT blends. This includes in-depth exploration of the techniques and conditions for manufacturing these films to meet specific mechanical and biodegradability requirements. The methodology will also detail the tests used to evaluate the properties of these films, such as tensile strength, elongation, impact resistance, and biodegradability, ensuring they comply with the EN 17033 standard. Furthermore, an evaluation method for the antibiotic adsorption capacity of the films is presented. This approach is critical in developing a BDM given the growing concern about antibiotic resistance and the potential role of agricultural practices in exacerbating the problem. The study will explore how different formulations of PLA/PBAT mixtures affect the adsorption of antibiotics, with the aim of developing films that do not lead to the accumulation of antibiotic resistance genes in the environment.

In summary, the methods section will present a comprehensive approach to the production of PLA/PBAT biodegradable films with a focus on optimizing

their performance for agricultural use while minimizing their environmental impact. The approach provides a foundation for study and the results found, where the methods are applied to produce and test BDMs.

CHAPTER 3

HYPOTHESES AND OBJECTIVES

This research addresses the following hypotheses and objectives:

Hypotheses:

1. PLA/PBAT blends can be produced in the lab that are uniform and reproducible in composition and thickness.
2. PLA/PBAT blends exhibit mechanical properties that are consistent with literature.
3. The addition of MCC and n-HA enhances the biodegradability of PLA/PBAT blends, thereby improving performance in agricultural applications.

Objectives:

1. To develop a laboratory-based methodology to produce PLA/PBAT blends, ensuring the process is reproducible, efficient, and yields consistent results.
2. To improve the composition of PLA/PBAT blends to maximize their utility in agricultural applications and improve their environmental benefits. Specifically, microcrystalline cellulose (MCC) and nanohydroxyapatite (n-HA) addition is expected to improve water absorption in PLA/PBAT blends.

CHAPTER 4

METHODS

This study outlines a comprehensive experimental procedure to develop and test biodegradable polymer composites as alternatives to conventional plastic films in agricultural applications, addressing the critical issue of microplastic contamination. This study involves the preparation and testing of PLA, PBAT, and PBAT/PLA blends using solvent casting and hot melt press methods. The tests include thermogravimetric analysis (TGA) for thermal stability, differential scanning calorimetry (DSC) for crystallinity, tensile strength testing, water absorption, UV aging. Additional studies in the future include durability under environmental conditions and antibiotic adsorption capacity, to evaluate the environmental impact of composites when used in agricultural settings such as wastewater treatment for irrigation. This comprehensive approach aims to determine the viability of these biodegradable composites as sustainable alternatives to conventional polyethylene films, focusing on their mechanical properties, biodegradability, and environmental safety.

PLA 4032D was purchased from Jamplast Inc, Ecoflex F Blend C1200 PBAT from BASF, the hydroxyapatite (20 nm) was purchased from Matexcel. Dichloromethane, cellulose, sulfamethoxazole (SMX) and ofloxacin (OFL) were purchased from Sigma-Aldrich.

4.1 Experimental Procedure

4.1.1 Solvent Casting and Hot Melt Press

All constituents are dissolved in dichloromethane (CH_2Cl_2) under completely mixed conditions for 24 hours (modified Yan et al., 2020 method, Table 4.1) in a closed beaker under a hood. The solution then undergoes sonication for 40 minutes. Solvent is evaporated from the beaker while continuously mixed resulting in a more viscous solution (30 min). The solution is then deposited as a cast film and placed in a plastic bag (small opening) allowing for the remaining solvent to evaporate slowly. The sample is dried at room temperature for 3 days with the plastic bag removed on the fourth day for 24 hours.

Table 4.1 Solvent Casting And Hot-pressed Blend Samples wt%

Sample name	wt%	
	PBAT	PLA
100 PBAT	100	0
100 PLA	0	100
30/70 PLA/ PBAT	30	70
20/80 PLA/PBAT	20	80
10/90 PLA/PBAT	10	90

Table 4.2 Solvent Casting Composite Samples wt%

Sample name	wt%			
	HA	PLA	PBAT	MCC
2 HA	2	83.7	9.3	5
4 HA	4	81.9	9.1	5
6 HA	6	80.1	8.9	5
4 MCC	6	81	9	4
6 MCC	6	79.2	8.8	6
7 MCC	6	78.3	8.7	7

PBAT/PLA blends are dissolved in dichloromethane (CH_2Cl_2) with same procedure as solvent casted sample and then dried in vacuum under 60 °C. The blend is cut with scissor into particles of 5 mm to 10 mm size. The hot melt press compresses the blend into a sheet by placing it under a pressure of 2 tons at 170 °C for 90 seconds for pure PLA and PLA/PBAT blends (Table 4.2), and 130 °C for 90 seconds for pure PBAT (modified Lyu et al., 2023 method). The film is held under a pressure of 0.0089 MPa and cooled to room temperature over a period of approximately 5 minutes, reducing the temperature from 170°C to 40°C with circulating room temperature water.

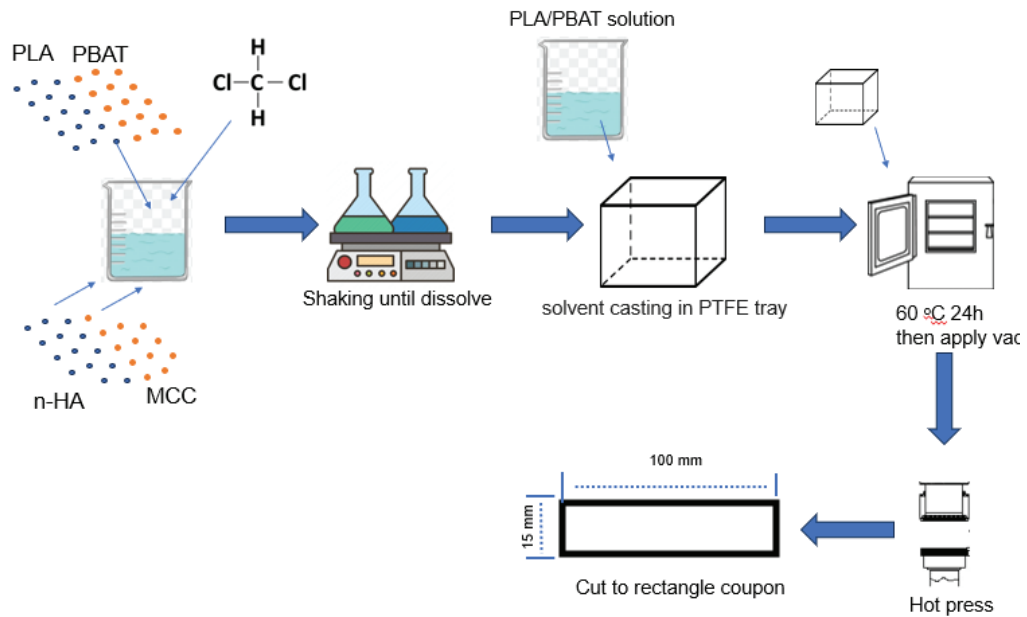


Figure 4.1 Experimental procedure modified from Yan et al. (2020).

Source: Yan, D., Wang, Z., Guo, Z., Ma, Y., Wang, C., Tan, H., & Zhang, Y. (2020). Study on the properties of PLA/PBAT composite modified by nanohydroxyapatite. *Journal of Materials Research and Technology*, 9(5), 11895–11904. <https://doi.org/10.1016/j.jmrt.2020.08.062>

4.2 Thermogravimetric Analysis (TGA)

Thermogravimetric analysis (TGA) was used to investigate the thermal stability of the film. Using 4 mg of sample, the temperature was raised from 30 °C to 600 °C at a heating rate of 10.0 °C/min. Nitrogen was used as the purge and protection (nitrogen) gas, and the flow rate of nitrogen was 20 mL/min (Yan et al. 2020).

4.3 Differential Scanning Calorimetry (DSC)

The DSC test addresses the crystallinity of the blend. Using 4 mg of sample, the temperature was raised from 30 °C to 180 °C at a heating rate of 10 °C

/min. The sample is cooled by liquid nitrogen from 180 °C to - 60 °C at a cooling rate of 10 °C /min. The nitrogen gas is used as the purge gas and the shielding gas. The gas flow rate is 20 mL/min (Sritham et al., 2018).

4.4 Tensile Test

The tensile strength and elongation properties of samples were tested using the CMT-5504 type capacity tester in accordance with GB/T 1040-2006. Each sample was cut into what is referred to as the dog bone shape from solvent casting films (ASTM D638) and 100 mm x 15 mm rectangle with the hot melt press films. These shapes reduce the influence of stress and slipping induced by loading grips (ASTM D882, Zhang et al., 2019). Before the tensile strength test is conducted, the cross-sectional area (thickness by width) is determined using a caliper. Tensile strength is calculated (Griffin et al., 2016) using the following equation:

$$S \left(\frac{kN}{mm^2} \right) = \frac{F(kN)}{a(mm^2)} \quad (1)$$

s is the tensile strength (MPa), F is the force required to break (kN), and a is the cross-sectional area (mm²)

4.5 Water Absorption Test

Water absorption analysis is used to investigate the polymer, blend, or composite's ability to absorb water (Yan et al., 2020). Water absorption through

the void space of a sample increases the degradation process through hydrolysis. When used as a film to promote crop yield, water absorption cannot exceed 10% to ensure its integrity (Tsou et al., 2022). However, once mulched into the soil, the biodegradation will be enhanced with increasing water absorption (> 4%) (Tsou et al., 2022). Samples were cut into 5 mm × 5 mm pieces and dried in a vacuum oven at 30 °C for 48 h. The dimensions of the sample are recorded along with the volume denoted as V (cm³). The original mass of dried sample is recorded, m₁ (g). The sample is then completely submerged in deionized water exposed to the atmosphere at room temperature where is maintained at 5, 7, and 8. The sample is then dried with wipes. The change in mass of the sample with water absorbed is measured and recorded as m₂ (g) at 24 h, 48 h, and 72 h, until there is no change in m₂ (Rahman et al., 2018). Water absorption (WA) is calculated as follows (Yan et al. 2020):

$$WA = ((m_2 - m_1)(g)) / (m_2(g)) * 100\% \quad (2)$$

4.6 UV Aging

UV aging was performed to evaluate the durability and stability of PLA/PBAT blends when exposed to UV light for extended periods of time. Samples were placed under the UV light in the hood to make sure air flow could remove all ozone generated by UV. The B100A/R UV lamp (Andwinski) intensity is 217 W/m² and wavelength of 365 nm. 95% of the UV is UV-A (315-400 nm

wavelength) (Albert et al., 2005). To simulate natural UV light exposure of Israel, similar to average wavelength of UV-A (358 nm) will be needed. Israel average sun irradiance is 2000 kWh/m²*year, and 5% of sun light is UV light; as a result, Israel average UV irradiance is 100 kWh/m²*year. The average growing period for crops is 4 months, which means the film need to be exposed to UV for 33.33 kWh/m². The total exposure time was calculated by the following formula (Gewert et al., 2018):

$$(33.33 \text{ kWh/m}^2) / (0.217 \text{ kW/m}^2) = 153.59 \text{ h} \quad (3)$$

The original weight is measured as m_1 and after aging, m_2 is the mass remaining. The equations presented are used to establish the relationship between UV aging performed in the laboratory and real-world UV exposure conditions, specifically with reference to solar irradiance levels in Israel.

4.7 Microplastic Preparation

Microplastic particles will be produced by grinding into smaller particles using mechanical grinder and then sieving to 3 to 5 mm.

4.8 Antibiotic Adsorption

Sulfamethoxazole (SMX) and ofloxacin (OFL) are the target antibiotics for the adsorption study (Seyoum et al., 2022). Adsorption experiments will include the optimized blend/composite, the control PE, and a blank condition as a function of antibiotic concentration and pH. A shaker (Thermo Fisher 88880023) will be

used to run multiple samples with completely mixed conditions (approximately 150 rpm) and with the required equilibration time (Guo et al, 2023). The concentration range of antibiotics is shown in Table 4.3 (Seyoum et al., 2022) (Figure 4.2). 0.01 M NaOH and HNO₃ will be used to maintain the pH 5.7, 7 and 8. Ionic strength will be an environmentally relevant conditions using 0.01 M NaNO₃ (Zhao et al., 2019). Adsorption will be calculated (Li et al., 2018) with

$$Q_t = (V(C_0 - C_t - A))/m \quad (4)$$

where Q_t (mg/g) is the adsorbed concentration, V (L) is the volume of aqueous solution, m (g) is the weight of the microplastic added (m/V is the loading), C_0 (mg/L) and C_t (mg/L) are the initial and equilibrium concentrations measured, respectively, and A is the blank concentration loss.

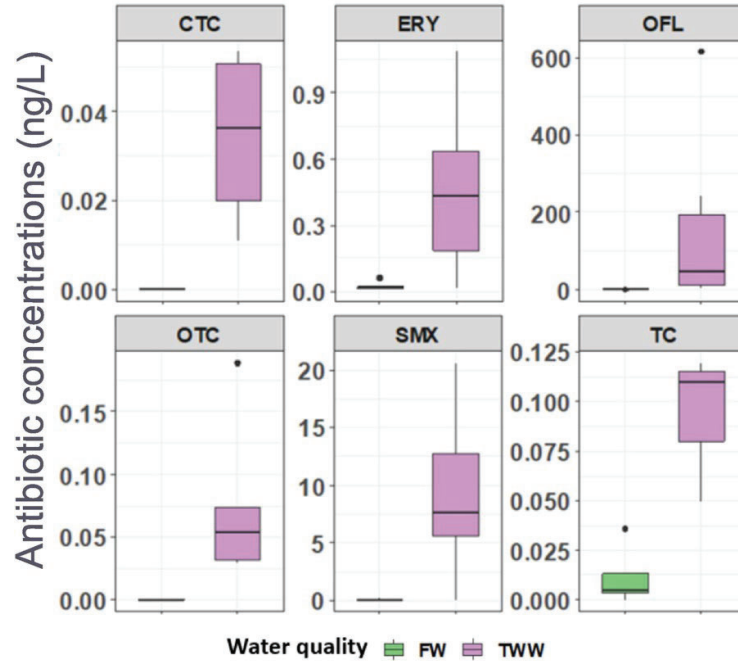


Figure 4.3 Antibiotic concentrations found in fresh water (FW) and treated wastewater (TWW) from Neve Ya'ar, Israel (Seyoum et al. 2022).

Source: Seyoum, M. M., Lichtenberg, R., Orlofsky, E., Bernstein, N., & Gillor, O. (2022).

Antibiotic resistance in soil and tomato crop irrigated with freshwater and two types of treated wastewater. *Environmental Research*, 211, 113021.

<https://doi.org/10.1016/j.envres.2022.113021>

Table 4.3 Concentrations To Be Used In The Study (Seyoum et al., 2022)

	Sulfamethoxazole (SMX)	Ofloxacin (OFL)
Fresh water concentration (ng/L)	0	0
Treated wastewater concentration (ng/L)	5 -- 12	10 -- 200
Concentration will be studied (ng/L)	5, 8.5, 12	67, 133, 200

Source: Seyoum, M. M., Lichtenberg, R., Orlofsky, E., Bernstein, N., & Gillor, O. (2022).

Antibiotic resistance in soil and tomato crop irrigated with freshwater and two types of treated wastewater. *Environmental Research*, 211, 113021.

<https://doi.org/10.1016/j.envres.2022.113021>

This chapter described the methods used in the study, including solvent casting and hot melt pressing processes. The preparation, formulation, and testing procedures of the polymer blends and composites are outlined to assess their viability as a sustainable alternative to polyethylene films. In the Results and Discussion Chapter results from the array of analyses are presented. This research demonstrates a protocol and methodology for developing an optimized biodegradable film for agricultural applications.

CHAPTER 5

RESULTS AND DISCUSSION

In this Results and Discussion Chapter, a systematic set of analytical methods are applied for determining the viability of a biodegradable film based on the EN 17033 standard (Plastics-Biodegradable mulch films for use in agriculture and horticulture Requirements and test methods, 2018.). Methods included mechanical, thermal properties, water absorption, and UV aging. Samples studied in this research involve standards and conditions assessed in literature: PLA, PBAT, and PLA/PBAT blends, and PLA/PBAT composites. This chapter addresses the effectiveness of the processing and methods used in developing a PE alternative.

5.1 Sample Preparation

During solvent casting, a significant challenge is the formation of air bubbles within the solution. This problem is mainly due to the high viscosity of the solution, which makes it difficult for bubbles to escape naturally. As the solution becomes increasingly viscous, trapped air bubbles are unable to rise to the surface and be released, causing defects in the final film. To solve this problem, a pre-evaporation step was introduced. This involves continuously stirring the solution while allowing some of the solvent to evaporate, thereby reducing the solvent concentration in the solution to a point where it is still

flowable but with few bubbles. This modification reduces the bubbles during drying, resulting in a smoother mixture with no visible air bubbles.

Although the bubble problem was solved, achieving uniform thickness across the entire film remained a challenge. Particularly problematic were the edges of the film, where tension during drying caused thickness changes. Even if the middle portion of the film is selected for analysis, it is difficult to consistently achieve the desired thickness. Several samples were produced, but the thickness could only be maintained within a certain range (Figure 5.1 A). To meet the requirements of ASTM D-638, hand-cut dog bone models were initially created using 3D printing (Figure 5.1 B). However, this approach resulted in a film with poor edge quality and cracks that did not meet the standards specified by ASTM D-638 (Table 5.1 and Figure 5.1 B).

The solvent casting method is not feasible for high-volume production and suffers from excessive drying times and unmanageable evaporation efficiency. The difficulty in achieving clean, precise cuts and inherent material limitations require the method to be re-evaluated. Given the challenges of achieving the required uniformity and quality via solvent casting, hot melt press was used to produce the films of the blends or polymers first produced by solvent casting. This method allows for greater control over film thickness and consistency,

resulting in greater compliance with ASTM standards and ensuring higher quality of the final product.

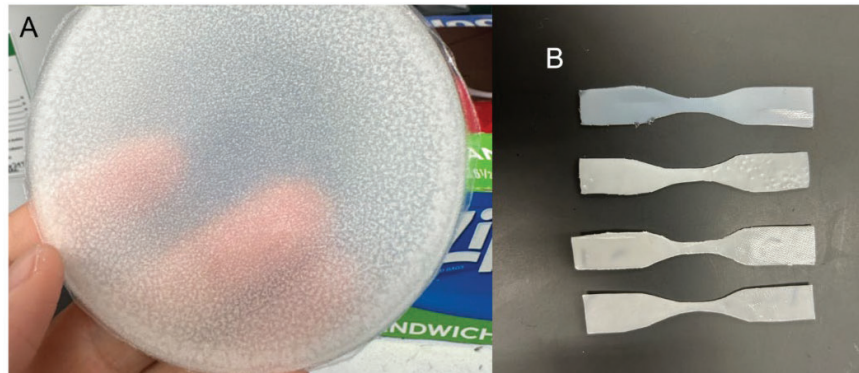


Figure 5.1 A) solvent casted sample, dots are air bubbles, B) Hand-cut samples.

Film uniformity and bubble formation were successfully resolved after transitioning from solvent casting to hot melt presses (Figure 5.2). However, this transition brought new challenges unique to the hot melt press process. Initially, using the melting point information from the PLA 4032D data sheet, the recommended processing temperature was 210°C. However, at this temperature, the mixture changed color to yellow and emits a burnt odor, indicating thermal degradation. The processing temperature was lowered to 170°C, effectively preventing thermal degradation and producing satisfactory blends.

Because molds are designed with different thicknesses, the hot melt press method allows for better control of film thickness (by purchasing molds of different thicknesses). This was particularly advantageous for producing films

that need to meet the EN 17033 elongation criteria for biodegradable mulches (BDM) (Table 5.1). The results show that films produced using this method show significant improvements in elongation properties, meeting the specifications of the EN 17033 standard. The ASTM D638 and ASTM D882 address analyses but do not address thickness requirements and mechanical property requirements; for film thicknesses less than 1 mm ASTM D882 must be used. This was particularly evident in the elongation at break test (discussed in mechanical test result section), where the films consistently met or exceeded the required percentage, demonstrating their suitability as biodegradable mulches.

In our experiments we explored various cooling rates (high rate: 22 °C/min, low rate: from 0.4 °C/min), pressures (0.0089 MPa, 0.0178 MPa, 0.0356 MPa) and temperature (170 °C, 190 °C, 210 °C) to understand their effects on film properties. We observed that rapid cooling significantly increases the brittleness of PLA-based blends, and regardless of the cooling rate, their brittleness is not sufficient to support high elongation. In contrast, the PBAT-hosted blends showed minimal sensitivity to different cooling rates. The amount of pressure has no effect on the performance of the film. The process of hot pressing is more like reshaping and expelling air bubbles and creating a more uniform surface. Regarding the temperature, the blend will not undergo thermal degradation if it does not exceed 190 °C.

Typical plastic mulch used in the USA ranges from 0.6 to 2.0 mils (0.0152 to 0.0508 mm) in thickness (Subrahmaniyan et al., 2012). As a result, the focus changed from ASTM D-638 standard to the ASTM D-882 standard (Table 5.1). However, the brass mod of the hot press machine cannot be cut when its thickness under 0.15 mm. Also, the size limitations of the hot melt press limited the maximum sample diameter to 13 cm, which is less than the 25 cm length recommended by ASTM D-882. This standard is designed to minimize the effects of fixture slip during tensile testing. Given the size of the samples, additional problems were encountered with the clamp slipping during tensile testing. The sliding affects the accuracy of the tensile strength measurements, thereby impacting the experimental setup.

Table 5.1 Standards

Standard	ASTM D638 Type 5	ASTM D882	Advantage: D882	EN 17033 requirements
Dimension	Length: 57.15 mm Width: 12.7 mm Thickness: variable	Length-to-width ratio 10:1	ASTM D882's flexible dimensions	Tensile stress >18 MPa
Thickness Requirement	materials >1 mm	thin films <1 mm	ASTM D882's thickness more fit mulch thickness	Thickness > 15 μ m
Sample Type	Molded or machined rigid samples	Thin films or sheets	ASTM D882 is designed for film	Tensile strain >350 %

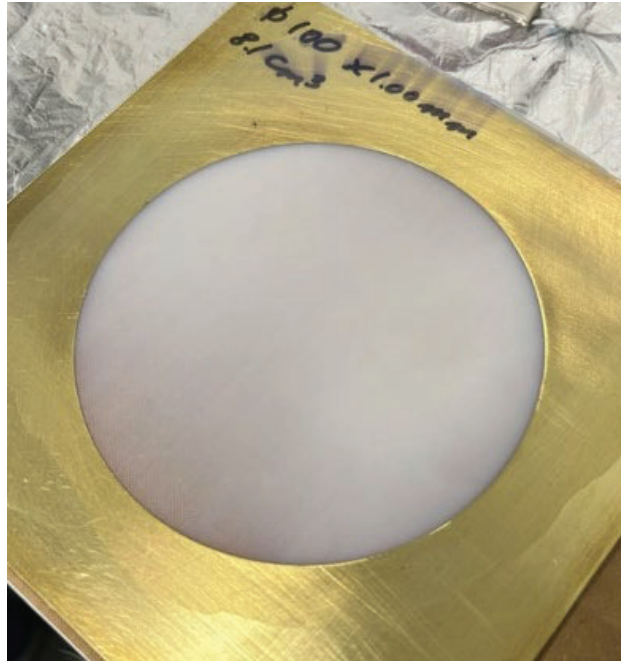


Figure 5.2 Hot melt pressed sample.

5.2 Mechanical Test

Tensile tests were conducted to evaluate the mechanical properties of PLA 4032D, PLA 4060D, PBAT, PBAT/PLA, and PLA/PBAT blends with and without n-HA and MCC present. Table 5.2 showed the properties from literatures and requirements of EN 17033 standard as the comparison.

Table 5.2 Polymer Blends Found In Literature And EN17033 Requirement

Sample name	Tensile stress break (MPa)	Tensile strain break (%)	EN17033 requirement for > 15 µm
PE ¹	22.1 – 31	11.2 - 12.9	Stress >18 MPa
PBAT ^{2,7}	16.42 - 21	670	
PLA ^{3,4,7}	48.82 - 59	3.81 - 7	
MCC ⁵	2.22-6.5	-	
PBAT/PLA blends			
90/10 PBAT/PLA ⁷	17.53	>600	Strain > 350%
80/20 PBAT/PLA ⁷	16.4	594.521	
70/30 PBAT/PLA ⁷	17.5	486.87	
9:1 ratio PLA/PBAT, 5 wt% MCC			
2HA ⁶	55	-	
4HA ⁶	50	-	
6HA ⁶	48	-	

All samples from Yan et al. (2020) have same ratio about 9:1 PLA/PBAT, sample name only show the wt% of HA, all samples from Lyu et al. (2023) show the wt% of PBAT/PLA.

Source:

¹Manufacturing, D., 2021. Polyethylene (HDPE/LDPE). <https://dielectricmfg.com/knowledge-base/polyethylene/>.

²Jian, J., Xiangbin, Z., Xianbo, H., 2020. An overview on synthesis, properties and applications of poly(butylene-adipate-co-terephthalate)–PBAT. *Advanced Industrial and Engineering Polymer Research* 3(1), 19-26. <https://doi.org/https://doi.org/10.1016/j.aiepr.2020.01.001>.

³Farah, S., Anderson, D. G., & Langer, R. (2016). Physical and mechanical properties of PLA, and their functions in widespread applications — A comprehensive review. *Advanced Drug Delivery Reviews*, 107, 367–392. <https://doi.org/10.1016/j.addr.2016.06.012>

⁴Ingeo™ Biopolymer 4032D Technical Data Sheet. (2002).

⁵Elsakhawy, M., Hassan, M., 2007. Physical and mechanical properties of microcrystalline cellulose prepared from agricultural residues. *Carbohydrate Polymers* 67(1), 1-10. <https://doi.org/10.1016/j.carbpol.2006.04.009>.

⁶Yan, D., Wang, Z., Guo, Z., Ma, Y., Wang, C., Tan, H., & Zhang, Y. (2020). Study on the properties of PLA/PBAT composite modified by nanohydroxyapatite. *Journal of Materials Research and Technology*, 9(5), 11895–11904. <https://doi.org/10.1016/j.jmrt.2020.08.062>, the ratio of each sample is wt% of n-HA/PLA/PBAT/MCC.

⁷Lyu, J. S., & Han, J. (2023). Scale-up fabrication of a biodegradable PBAT/PLA composite film compatibilized with a chain extender for industrial agricultural mulch film application. *Composites Part C: Open Access*, 12, 100397. <https://doi.org/10.1016/j.jcomc.2023.100397>.

5.2.1 Pure Samples

Pure PLA and PBAT are the only materials studied that exhibit the required transverse tensile strength of 18 MPa (Samples 1, 2, 3, and 4; Table 5.3; Figures 5.3 and 5.4). However, the degradation rate of pure PBAT cannot meet agricultural plant growing period requirements (Jian et al., 2020). Fu et al. (2020) reported that pure PBAT exhibited excellent tensile strength after 6 months of use. Although discolored and cracked during the growing season, the decay process may take more than six months. In Table 5.3 and Figure 5.3, the samples marked with an asterisk represent the use of PLA 4060D. According to test data, mechanical properties are slightly different from PLA 4032D. Because PLA 4032D exhibits greater ductility and impact resistance, PLA 4060D is not as competitive and is not recommended. Both Samples 1 and 2 (Table 5.3) have a high tensile strength of 48, but their relatively low percentage of strain fracture indicates that they are strong but not very ductile. Samples 3 and 4 (Table 5.3, Figure 5.4) are both 100% PBAT and show different properties. Sample 3 exhibited an extremely high strain fracture (>1000%) (0.43 mm thickness) with excellent ductility and did not fracture

during the test. Sample 4 with a 0.13 mm thickness showed a stress fracture of 23.7 MPa and a high strain fracture of 368.1 %; both of which are above EN 17033 requirements (Table 5.2). Pure PBAT exhibits similar properties to commercial PE films (Sample 5, Table 5.3), demonstrating that PBAT/PLA films can be a potential alternative to PE if the degradation time can be increased by blending with PLA.

Table 5.3 Result Of Mechanical Test

Sample number	Sample name	Thickness (mm)	Stress break (MPa)	Strain break (%)	ASTM test method
9	100PLA	0.25	48.48 ± 7.26	4.04 ± 0.29	D882
2	100PLA*	0.46	47.03 ± 0.91	2.33 ± 0.23	D882
3	100PBAT	0.48	-	> 1000	D882
4	100PBAT	0.13	23.7 ± 2.72	368.1 ± 19.6	D882
5	PE	0.1	21.28 ± 2.51	> 1000	D882

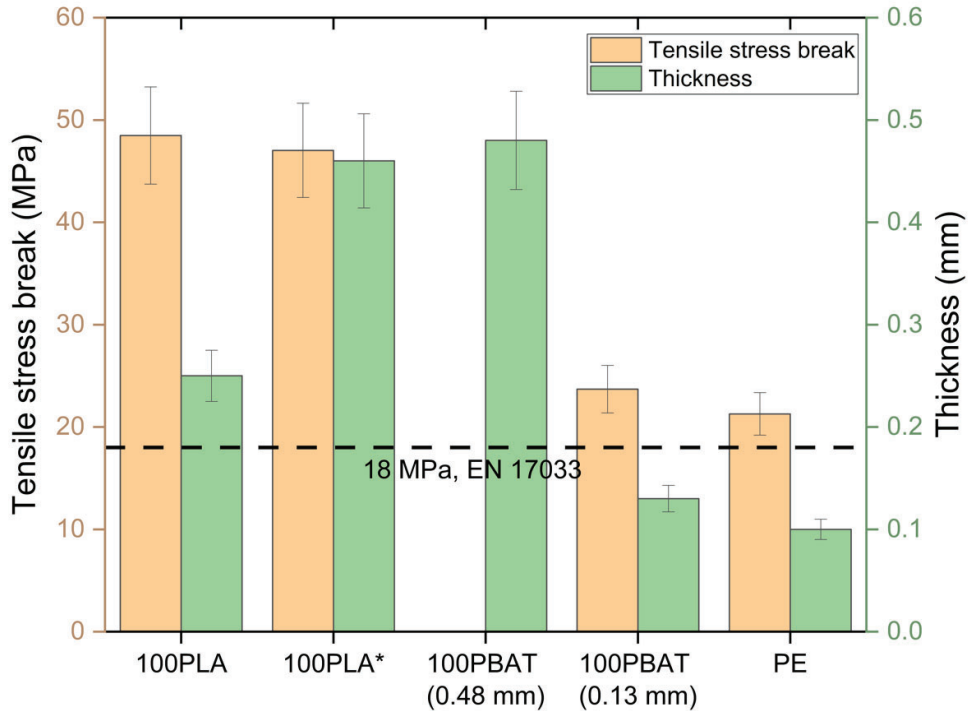


Figure 5.3 Tensile stress result of composites with EN 17033 reference line. Please refer to Table 5.3 for sample definition. Sample 3 didn't break during tensile test, so there is no tensile stress break data.

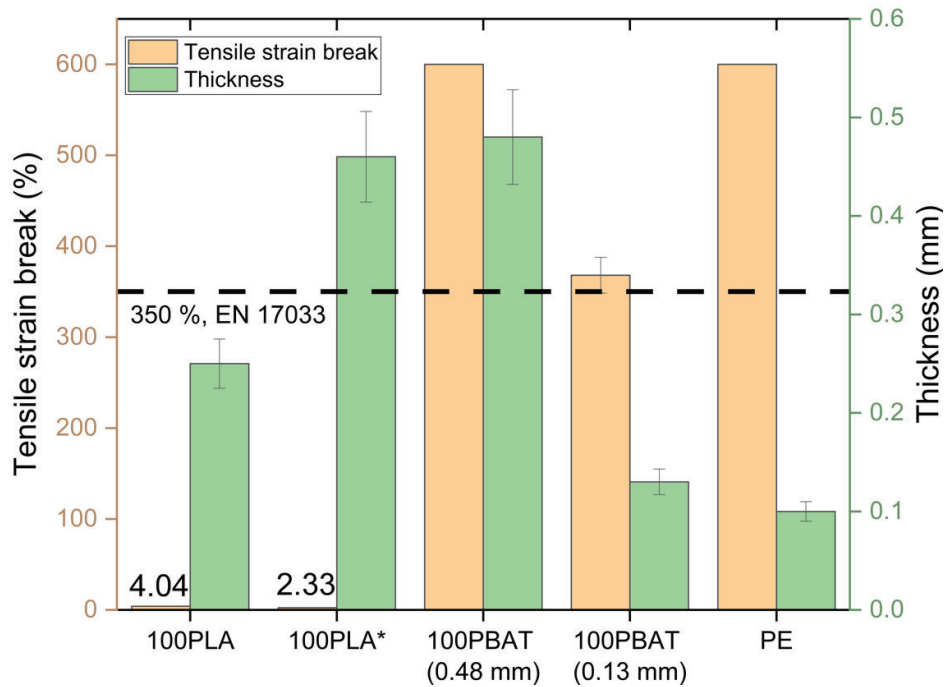


Figure 5.4 Tensile stress result of composites with EN 17033 reference line. Please refer to Table 5.3 for sample definition.

5.2.2 PBAT/PLA Blends

Figures 5.5 and 5.6 show the relationship between tensile strain and stress at break with sample thickness. As the thickness of the specimen increases, the force exerted to break the material increases while reducing edge effects because the amount of material capable of carrying the load increases. The sliding (zigzag, Figure 5.7) that occurred in sample 9 which reduced the tensile stress and was caused by the sample not being properly clamped within the testing equipment. Sample 3b did not slip during the initial part of the test and had higher tensile stress, indicating better adhesion to the test equipment, but eventually slipped and could not be prevented even with tape fixation (Figure 5.7). Equipment limitations can only be solved by replacing equipment with other models.

The ASTM D882 standard specifies a certain aspect ratio and gap (10:1, 28 cm) between anchors to minimize edge effects and slippage. However, due to the size limitations of the hot melt press, the same size sample as Zhang et al. (2019) was used (10 cm x 1.5 cm, 5 cm gap), which is one of the reasons why the mechanical test results are potentially affected. The obvious slip and smaller stress in Figure 5.7 also prove the influence of slip and edge effects.

When comparing the tensile stress results with those reported by Lyu et al. (2023) (Table 5.2). In Table 5.2 we note that the differences may be attributed

to the different PLA grades used. Samples 6 and 7 (Table 5.4) containing PLA 4032D showed different stress behavior and lower elongation compared to the results of Lyu et al. (2023) (Table 5.2), which may be due to the differences between PBAT and the specific PLA grade in our blends. The difference between high strain and low tensile strength in the blend indicates a complex interaction between the two polymers. Although the addition of PBAT hosted samples enhanced flexibility, the results indicate the need for further optimization to balance scale and thickness to meet the EN 17033 standard.

We tested two thickness to prove the edge effect and slipping problem (Sample 8 and 9, Table 5.4). The increase in elongation confirms that thickness affects elongation to a certain extent. This is also consistent with the observations of Yang et al. (2013). The reduction in sample thickness and roughness of the surface and cut surfaces can lead to stress concentrations at the edges during tensile testing, resulting in premature failure or lower measured tensile strength. This effect is more pronounced in thinner samples, where the actual tensile strength of the material should be higher than the measured value. Although all samples do not meet the tensile stress required by EN 17033 (Table 5.2), Sample 3b (less sliding) offers us the possibility to obtain a higher tensile stress, and Sample 9 already far exceeds the elongation required by EN 17033 (Figure 5.7). In future work, it is necessary to replace

more advanced equipment and increase the size of the material to meet the requirements of ASTM D882.

Table 5.4 Result Of Mechanical Test

Sample number	Sample name	Thickness (mm)	Stress break (MPa)	Strain break (%)	ASTM test method
6	70/30 PBAT/PLA	1.15	7.79 ± 0.52	16.85 ± 3.23	D638
7	80/20 PBAT/PLA	0.23	7.68 ± 0.48	83.05 ± 18.97	D638
8	90/10 PBAT/PLA	0.18	7.44 ± 1.03	273.27 ± 60.65	D882
9	90/10 PBAT/PLA	0.48	7.43 ± 0.50	427.46 ± 50.67	D882
10	70/30 PBAT/PLA*	0.22	7.82 ± 0.69	15.27 ± 2.94	D882
11	80/20 PBAT/PLA*	0.21	8.47 ± 0.72	155.42 ± 63.84	D882
12	90/10 PBAT/PLA*	0.22	8.63 ± 0.52	248.24 ± 35.73	D882

Sample names with asterisk (*) after PLA mean using PLA 4060D instead of PLA 4032D.

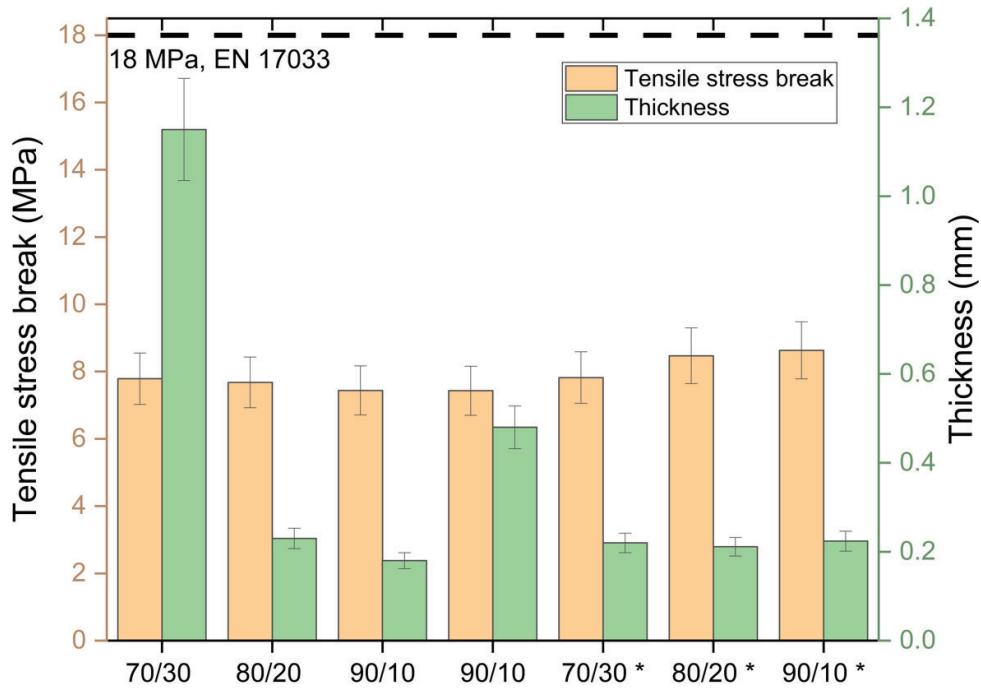


Figure 5.5 Tensile stress result of composites with EN 17033 reference line. Please refer to Table 5.2.2.1 for sample definition.

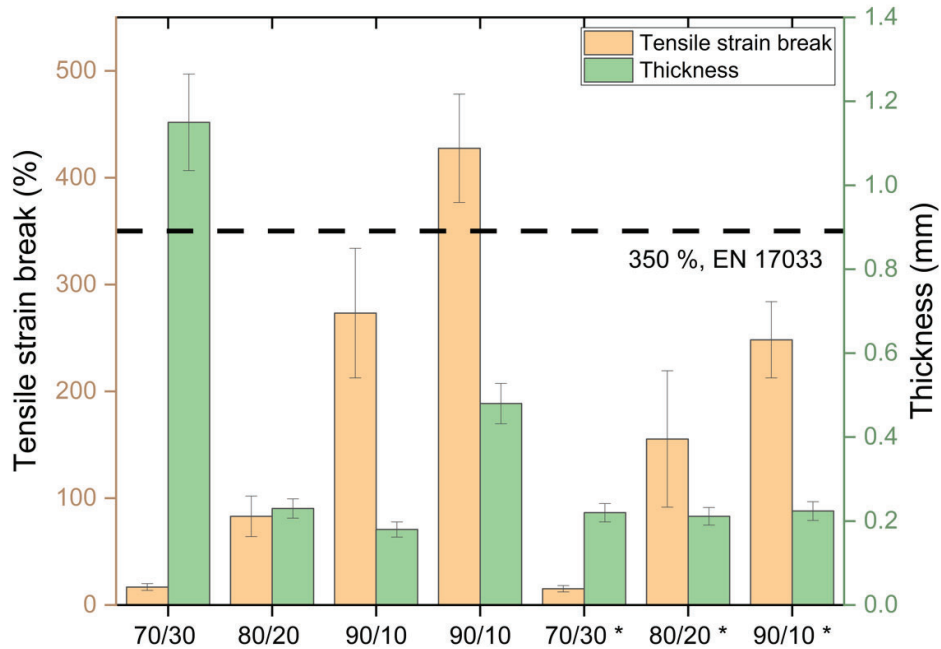


Figure 5.6 Tensile stress result of composites with EN 17033 reference line. Please refer to Table 5.2.2.1 for sample definition.

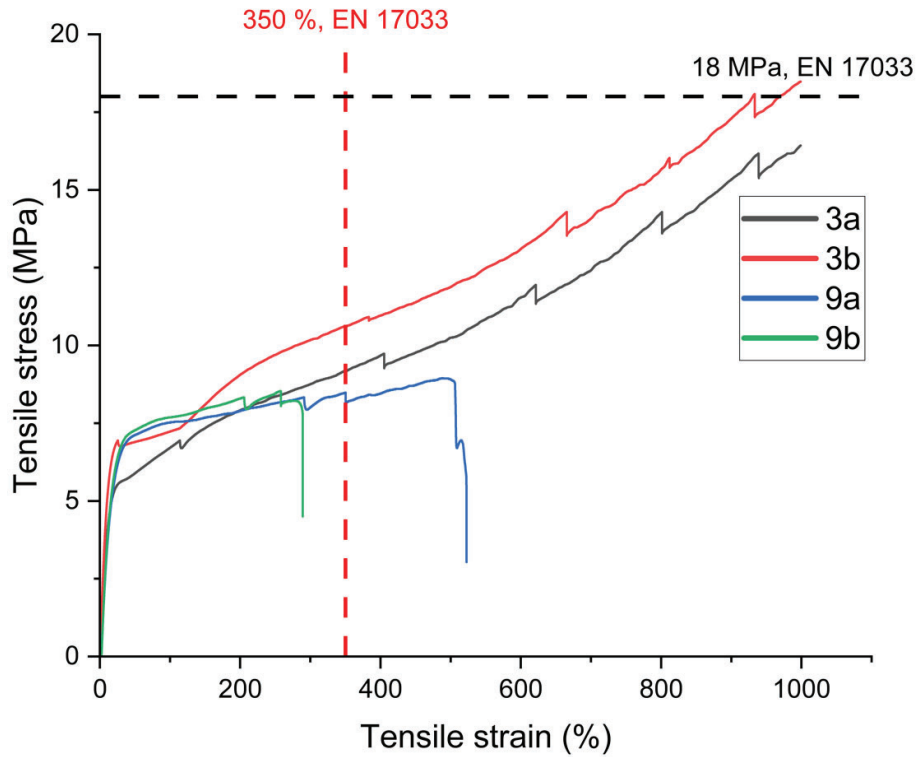


Figure 5.7 Tensile strain vs tensile stress plot by sample 3 and sample 9. Please refer to table 5.3 and table 5.4 for sample definition.

5.2.3 PBAT composite

The results (Table 5.5, Samples 15 to 18) show a general trend of decreasing tensile stress with increasing concentrations of n-HA and MCC. Specifically, the tensile stress ranges from 58.49 MPa in Sample 13 to 37.55 MPa in Sample 18. These tensile stresses significantly exceed the standards specified in EN 17033 (consisting mainly of PLA, Table 5.2, Figure 5.8). However, the strain percentages of these samples are lower, ranging from 1.16% to 4.71%, significantly below the requirements of the EN 17033 standard (Figure 5.9). This lower strain percentage highlights the limits of ductility, which is critical for

agricultural applications as the material must withstand various mechanical stresses without failure.

Comparing the results of Yan et al. (2020) (Table 5.2) on the mechanical properties of PLA/PBAT blends with n-HA and MCC revealed interesting similarities and differences. Yan et al. (2020) describes in detail how the addition of n-HA affects mechanical properties, focusing mainly on its effects on crystallinity and tensile strength. They noted that the addition of n-HA significantly increased the crystallinity of the composites and that its uniform dispersion at lower proportions improved the overall performance of the material. This outcome is consistent with the observation that tensile strength decreases with increasing n-HA concentration. For example, in our Sample 18, with lower n-HA and MCC concentrations, a tensile strength of 58.49 MPa was observed, the same high strength observed in the sample of Yan et al. (2020); in contrast, the tensile strength of Sample 15 with higher a concentration dropped to 48.83 MPa. This decrease is also consistent with the results of Yan et al.: increasing additive concentration resulted in a decrease in strength.

Comparing Figures 5.10 and 5.7, it is very easy to find that the elongation of the composite after changing PLA as the main component decreases sharply. A small amount of PBAT addition cannot make PLA be a competitor of BDM, and the addition of MCC and n-HA will cause a small decrease in tensile

strength, but MCC and n-HA must be added as the main water absorbent part of the material. A key point among the findings is the impact of MCC on material properties. The data shows that samples with greater MCC concentrations (such as Samples 17 and 18) exhibited a decrease in tensile strength. Yan et al. (2020) concluded that while MCC and n-HA act as nucleating agents, the hydroxyl groups cause agglomeration of particles resulting in poor interactions with PLA/PBAT. Adding too great a concentration of nucleating agent can lead to a decrease in crystallinity because too many fibers can form gaps inside the film (Lay et al., 2019) and increase the elongation at break (El-Hadi, 2017). Although adding MCC can increase the elongation, it can also reduce the tensile stress. This inverse relationship poses a challenge to meet the EN 17033 standard, which requires a balance between strength and ductility for effective function in agricultural environments. Our data show that although increasing MCC concentration improves ductility, it does not reach the levels specified by the EN 17033 standard. This result suggests that while the ductility of the material can be tuned by adjusting the MCC concentration, the current PBAT/PLA ratio in our experiments may not be fully optimized for the harsh conditions of agricultural applications.

Table 5.5 Result of mechanical test

Sample number	Sample name	Thickness (mm)	Stress break (MPa)	Strain break (%)	ASTM test method
13	2 HA	0.07	58.49 ± 4.81	1.16 ± 0.02	D638
14	4 HA	0.06	50.60 ± 13.32	1.25 ± 0.21	D638
15	6 HA	0.05	48.83 ± 2.87	1.75 ± 0.11	D638
16	4 MCC	0.06	44.58 ± 1.64	1.35 ± 0.13	D638
17	6 MCC	0.06	39.06 ± 2.04	3.45 ± 0.32	D638
18	7 MCC	0.06	37.55 ± 2.77	4.71 ± 0.18	D638

Samples 13 to 15 have same ratio of 9:1 PLA/PBAT and 5 wt% of MCC, samples 16 to 18 have same ratio of 9:1 PLA/PBAT and 6 wt% of HA, sample names are wt% of HA and MCC addition.

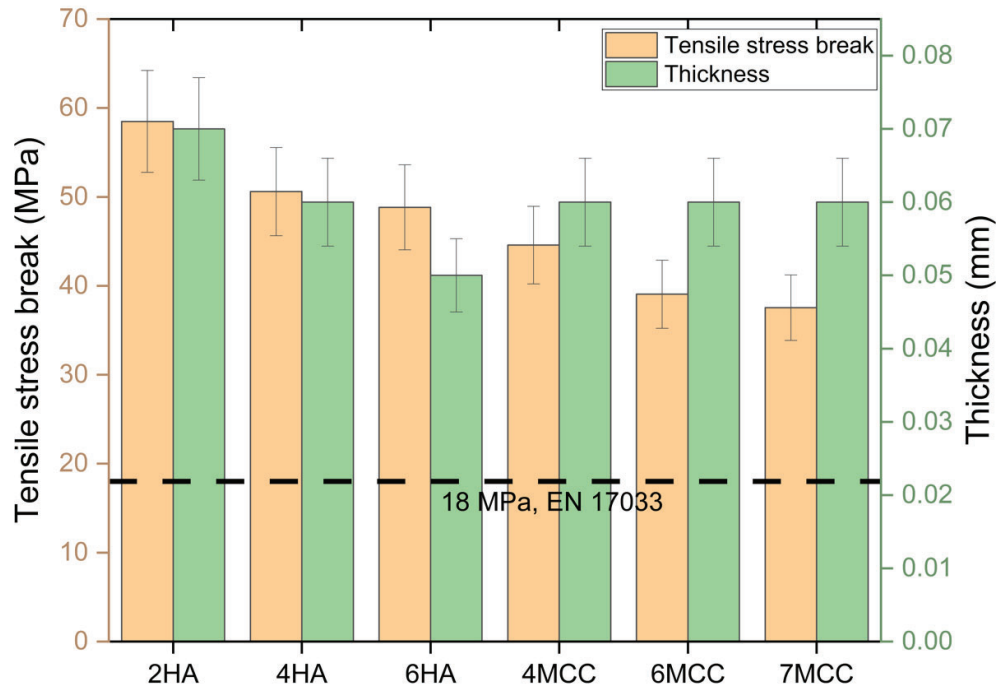


Figure 5.8 Tensile stress result of composites with EN 17033 reference line. Please refer to Table 5.5 for sample definition.

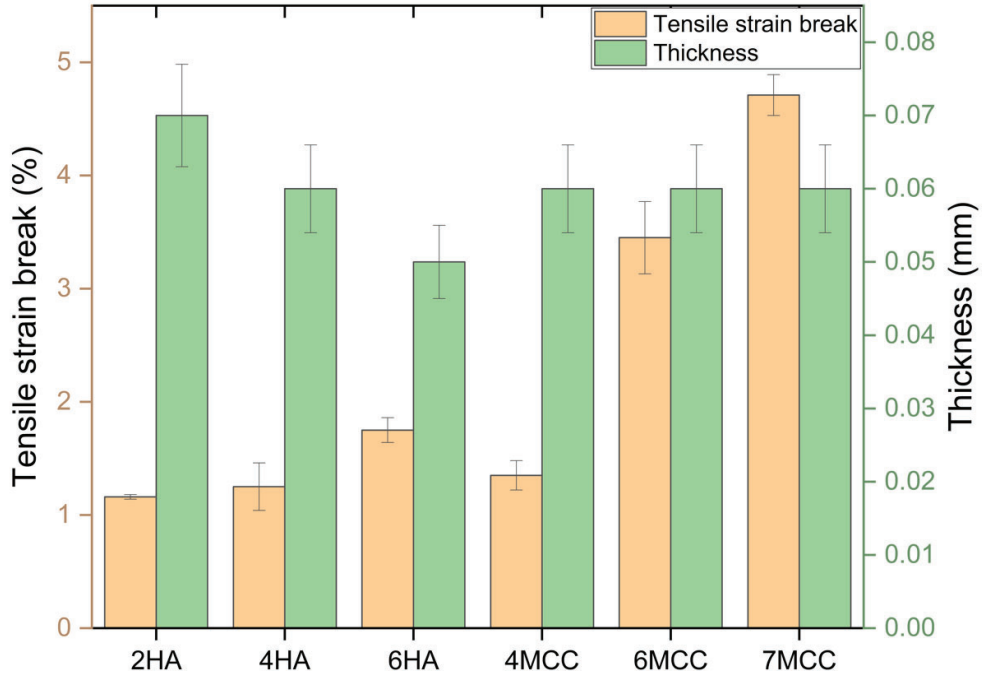


Figure 5.9 Tensile strain results of composites. Please refer to Table 5.5 for sample definition.

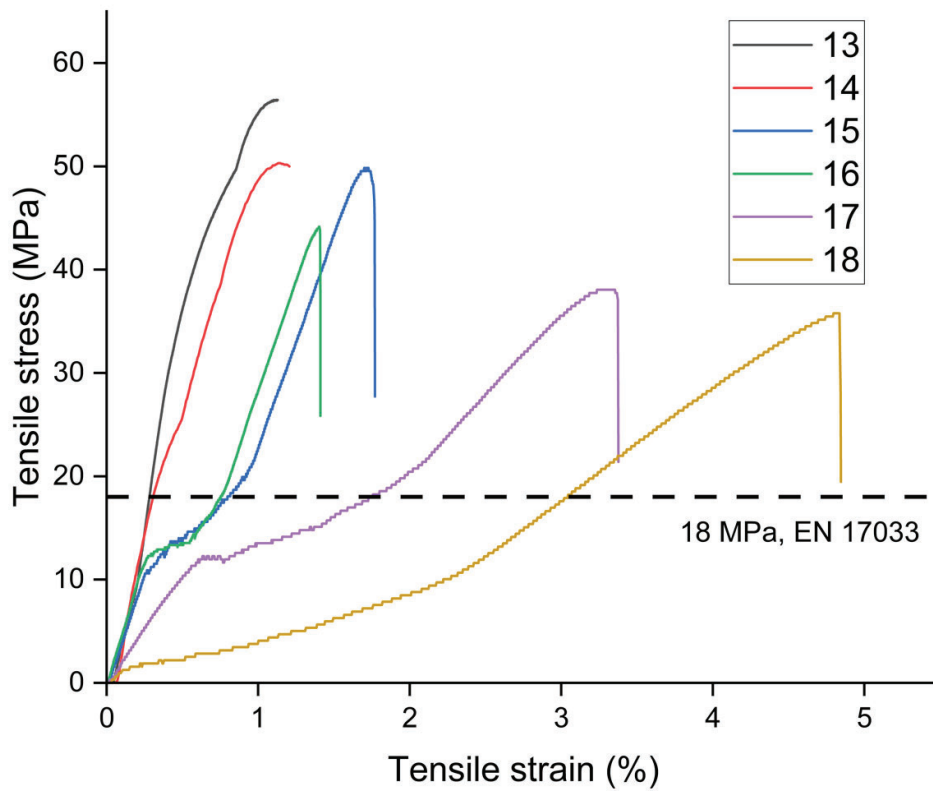


Figure 5.10 Stress vs Strain plot of Samples 13 to 18. Please refer to Table 5.5 for sample definition.

In a comprehensive analysis of pure PLA and PBAT samples, PBAT/PLA mixtures, and PBAT/PLA composites containing additives such as n-HA and MCC, several key findings related to the EN 17033 standard emerged. Pure PLA and PBAT materials exhibit the required tensile strength of 18 MPa and pure PBAT complies with the EN 17033 standard, but the degradation rate of PBAT poses challenges for agricultural applications. Due to the addition of PLA, the PBAT/PLA blend achieved the elongation required by EN 17033, but due to limitations of production and testing equipment, the tensile strength did not meet the standard. In the case of PBAT/PLA composites, although the incorporation of n-HA and MCC additives significantly increases the tensile strength, often exceeding the EN 17033 requirements, these composites hardly meet the elongation requirements of the standard. Future experiments should pay more attention to the PBAT/PLA ratio and find ways to avoid slippage.

5.3 Thermal Test

5.3.1 Thermogravimetric Analysis (TGA)

The thermal decomposition behavior of PBAT/PLA blends and their pure components was scrutinized, with specific emphasis on the influence of post-processing techniques and blend composition. The samples subjected to tensile testing and those casted from solvent, both composed of a 90/10 PBAT/PLA blend (Table 5.6), displayed decomposition starting temperatures of

339.75 °C and 342.58 °C, respectively, alongside onset decomposition temperatures at 412.08 °C and 411.08 °C. This contrasted with the behavior of pure PLA and PBAT samples, which exhibited lower and higher decomposition starting temperatures at 334.7 °C and 363.8 °C, respectively. Notably, pure PLA showed a markedly higher char yield of 0.09 %, compared to 5.83 % in pure PBAT, indicating significant differences in thermal stability and residue formation.

The results align with those reported by Xiang et al. (2020), who evaluated PLA content in PLA/PBAT blends using TGA. The onset decomposition temperatures of our blends sit comfortably within the range reported in their study, confirming the reliability of our thermal analysis. Moreover, the higher decomposition temperatures observed in our samples after tensile testing and solvent casting may be indicative of increased interaction between PBAT and PLA molecules, possibly due to the mechanical or solvent-induced rearrangement of polymer chains.

Furthermore, the observation that hot-pressed samples exhibit higher DTG peak temperatures (Figure 5.11), as noted by Jeya et al. (2023), suggests enhanced crystallinity in these samples. This finding could explain the increased thermal stability in our tensile-tested samples, assuming a similar mechanism is at play. The correlation between processing methods,

crystallinity, and thermal behavior underscores the complexity of polymer blend behavior and the pivotal role of post-processing conditions in defining material properties.

This analysis not only corroborates existing literature but also expands our understanding of the thermal characteristics of PLA/PBAT blends. It underscores the need for careful consideration of processing conditions in tailoring the thermal properties of polymer blends for specific applications.

Table 5.6 Thermogravimetric Analysis for PBAT/PLA 90/10 Blend

Sample Type	Decomposition Starting Temperature (°C)	Onset Decomposition Temperature (°C)	Char Yield (%)
Hot pressed	339.75	412.08	4.59
Solvent Casted	342.58	411.08	5.02
100 PLA	334.71	3841	0.991
100 PBAT	363.81	4201	5.831

Sources: 1Xiang, S., Feng, L., Bian, X., Gao, L., & Chen, X. (2020). Evaluation of PLA content in PLA/PBAT blends using TGA. *Polymer Testing*, 81, 106211.

<https://doi.org/10.1016/j.polymertesting.2019.106211>

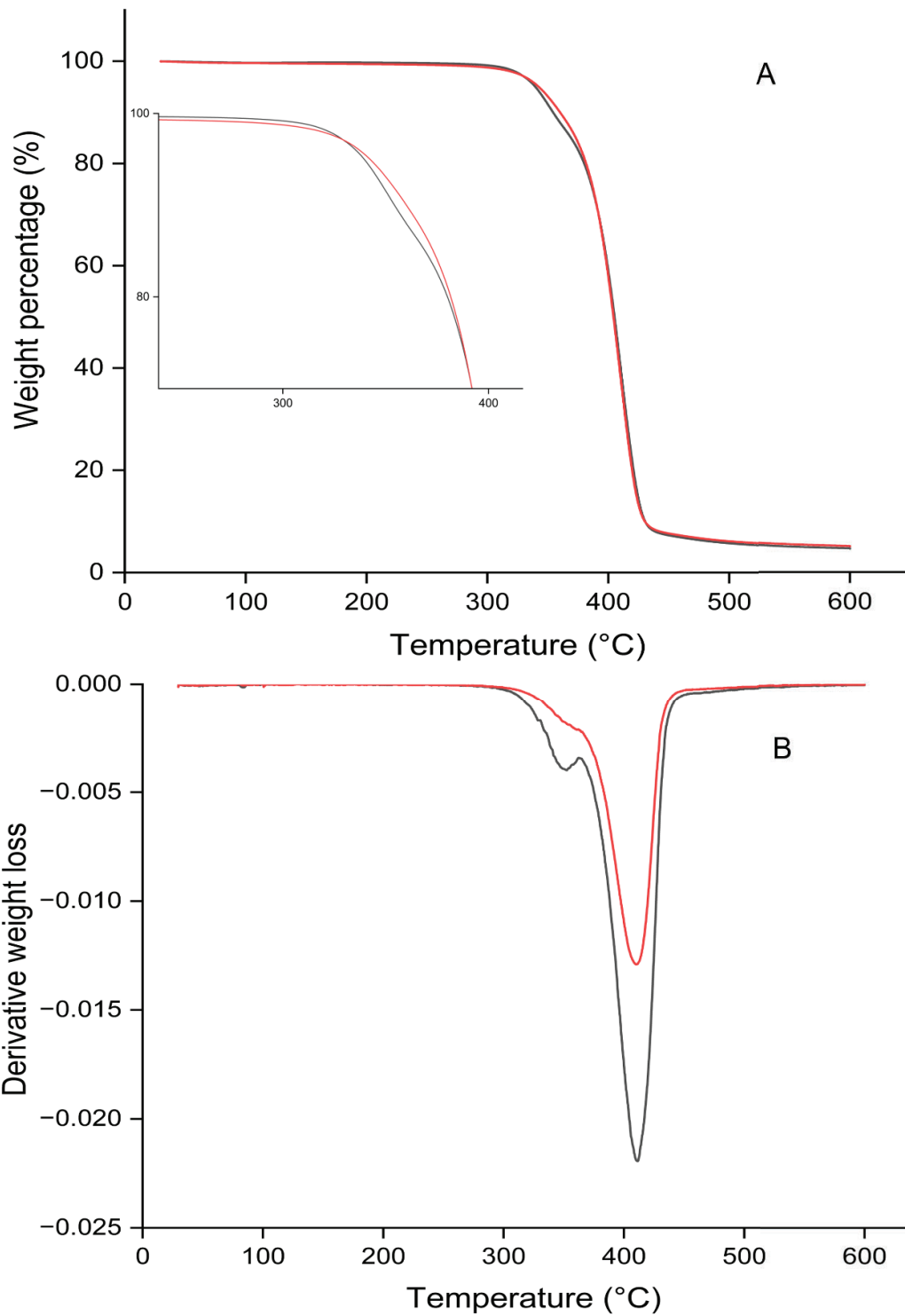


Figure 5.11 A) TG curve of PLA/PBAT 10/90 blend, B) Derivative of PLA/PBAT 10/90 blend, red line is hot press sample, black line is solvent casted sample.

5.3.2 Differential Scanning Calorimetry (DSC)

The DSC and TGA analyses provide complementary insights into the thermal properties and crystalline behavior of PLA/PBAT blends. From the DSC analysis (Table 5.7), the crystallinity (X_c) of PLA in the solvent-casted sample was found to be 25.96%, which increased to 37.40% after tensile testing. This increase in crystallinity can be attributed to the alignment and reorganization of polymer chains during the tensile testing process, promoting a more ordered structure. In contrast, the crystallinity of PBAT decreased marginally from 6.07% in the solvent-casted sample to 5.82% after tensile testing.

TGA data further elucidated these findings. Generally, materials with higher crystallinity exhibit higher thermal stability (Jeya et al. 2023). This is evident in PLA assemblies where an increase in crystallinity after tensile testing corresponds to a higher decomposition temperature as observed in TGA analysis. This indicates that mechanical stress during tensile testing not only enhances crystallinity but also improves the thermal stability of the PLA component in the blend.

However, the slight decrease in PBAT crystallinity after tensile testing seems counterintuitive since increased crystallinity leads to increased thermal stability. This may be due to inherent structural differences between PLA and PBAT. PBAT is known for its flexibility and lower glass transition temperature

compared to PLA. The mechanical forces applied during tensile testing may cause the destruction of crystalline regions in PBAT, resulting in a slight decrease in crystallinity. However, this reduction is relatively small and does not significantly affect the overall thermal stability of PBAT observed in TGA.

Table 5.7 Thermal Parameters From 2nd Heating Scan Of Differential Scanning Calorimetry (DSC) Analysis

PLA	ΔH_m (PLA), J/g 167.9°C	ΔH_m (100% Crystalline PLA), J/g	w/w PLA	X _c (PLA), %
Solvent casted 90/10 PBAT/PLA	2.4145	93 ¹	0.1	25.96
Hot pressed 90/10 PBAT/PLA	3.4779	93 ¹	0.1	37.40
PBAT	ΔH_m (PBAT), J/g 121.4°C	ΔH_m (100% Crystalline PBAT), J/g	w/w PBAT	X _c (PBAT), %
Solvent casted 90/10 PBAT/PLA	6.2275	114 ²	0.9	6.07
Hot pressed 90/10 PBAT/PLA	5.9688	114 ²	0.9	5.82

Sources: ¹Aliotta, L., Sciara, L. M., Cinelli, P., Canesi, I., & Lazzeri, A. (2022). Improvement of the PLA crystallinity and heat distortion temperature optimizing the content of nucleating agents and the injection molding cycle time. *Polymers*, 14(5), 977. <https://doi.org/10.3390/polym14050977>

²Bastarrachea, L. J., Dhawan, S., Sablani, S. S., Mah, J., Kang, D., Zhang, J., & Tang, J. (2010). Biodegradable Poly(butylene adipate-co-terephthalate) Films Incorporated with Nisin: Characterization and Effectiveness against *Listeria innocua*. *Journal of Food Science*, 75(4). <https://doi.org/10.1111/j.1750-3841.2010.01591.x>

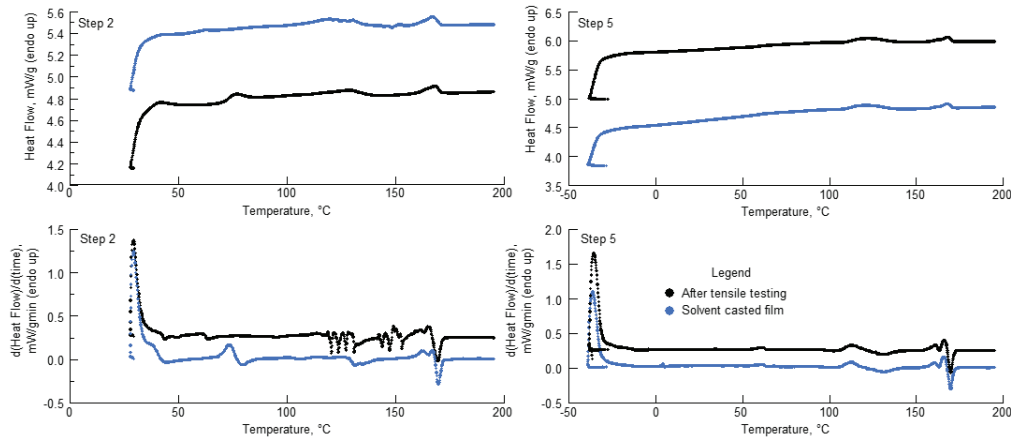


Figure 5.12 DSC result of PBAT/ PLA 90/10 blend, Step 2 is the first heating, Step 5 is the second heating.

5.4 Water Absorption

This study carefully evaluated a range of samples, from control to new blends, as described in Figure 5.13. This data reflects the water adsorption capacity of samples with different compositions at different pH levels. This trend indicates that the average water adsorption amount generally increases with the addition of n-HA and MCC, which is consistent with Yan et al. (2020), and they reported that the addition of 8 % n-HA achieved the maximum water absorption.

However, due to differences in experimental methods, Yan et al. (2020) only tested the water absorption of the sample for 24 hours, and the extended immersion time in the experiment was an important variable that resulted in higher water absorption compared to the shorter duration used by Yan et al. This result indicates that these materials will continue to absorb water after 24 hours, which is critical for applications where long-term exposure to moisture is expected.

Comparing the samples with different MCC concentrations, it was observed that the sample with 6 % MCC showed the greatest water absorption capacity, which may be due to the optimal concentration of MCC providing a balance between porosity and structural integrity, promoting water uptake. Input amount, and both n-HA and MCC have many hydroxyl groups, which can also increase water absorption. The water absorption capacity of hydroxyl-containing materials, such as MCC and n-HA, is significantly affected by the pH of their environment.

Experiments show that while the addition of hydroxyl-containing compounds such as MCC and n-HA generally increases the water absorption capacity of PBAT/PLA blends, there is a complex interaction between the concentration of these compounds and the material structure. The decrease in water absorption observed in Sample 7 MCC suggests that there is an optimal concentration of MCC that ensures maximum water absorption, beyond which the effect may have a negative impact on the material's ability to absorb water. This research needs to be expanded in the future to include controls such as other BDMs and PE microplastics. The water absorption and other work with environmental chambers needs to be compared to irrigation green house experiments.

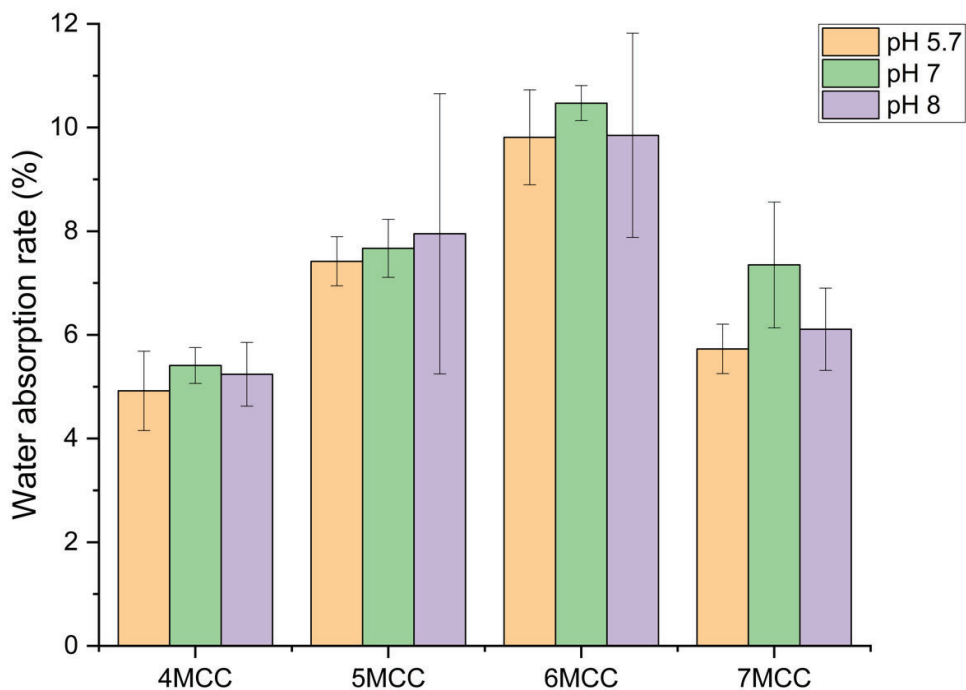


Figure 5.13 Water absorption results of PLA majority samples, Samples 4MCC, 5MCC, 6MCC, and 7MCC have same ratio of 9:1 PLA/PBAT and 6 wt% of HA. Sample names are wt% of HA or MCC addition.

5.5 UV Aging

In UV aging experiment, Samples 8 to 11 (Figure 5.14) were exposed under UV light for 153 hours, with continuous air flow to remove ozone generated by UV light. After aging, there is a relatively low loss of mass. As shown by the percentage of weight loss, the UV aging process applied to our samples produced a modest change in quality. This outcome indicates the relatively stable behavior under UV exposure, which is promising for applications where material life under sunlight is critical. In the study by Ludwiczak et al. (2023), they measured 4-month mass change in a 70/30 PLA/PBAT blend and found no mass change in the sample consistent with our Samples 8 to 11. With the

increasing MCC, the percentage of mass loss shows an upward trend, which may indicate that MCC slightly increases the photodegradation efficiency under ultraviolet light.

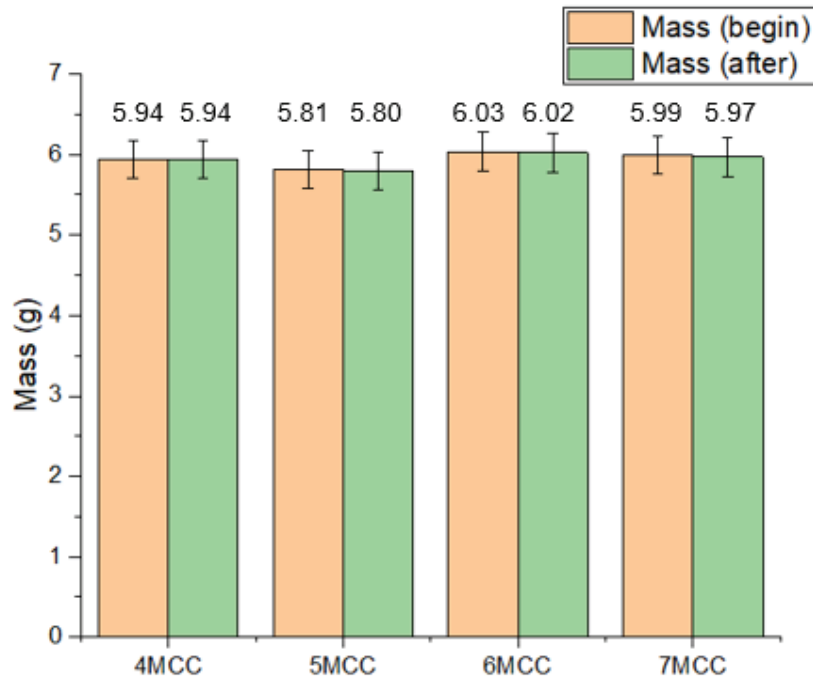


Figure 5.14 Mass loss during UV aging of PBAT/PLA composite

In this chapter, the mechanical properties and thermal stability of PLA/PBAT blends were investigated, demonstrating their potential as an effective alternative to traditional polyethylene (PE) films in agricultural applications. The results suggest that while blending PBAT with PLA can improve flexibility, it does present challenges in maintaining tensile strength and requires further optimization to comply with the EN 17033 standard for biodegradable mulch. n-HA and MCC have a particularly significant effect on

improving mechanical properties and water absorption. The study, which combined DSC and TGA data, showed that using the hot melt press after solvent casting can increase the crystallinity of these materials, potentially improving their mechanical properties. Water absorption tests and UV aging demonstrated that the addition of n-HA and MCC increased water absorption as well as the superior stability of the mixture under sunlight. However, meeting all requirements of the EN 17033 (Table 5.2) standard is a daunting challenge. The discussion in this study suggests that a full factorial study is needed to improve the composition and processing conditions of PLA/PBAT blends. Adjusting these parameters is essential to tailor the mechanical properties of these mixtures to specific agricultural applications, thereby contributing to the development of more sustainable and environmentally friendly agricultural application.

CHAPTERT 6

CONCLUSION AND FUTURE WORK

This research addressed the methodology in developing and accessing films for agriculture applications. Solvent casting followed by hot melt press resulted in films with uniform and consistent thickness, composition, and behavior.

Mechanical and behavior and thermal properties are critical analyses for PBAT/PLA blends with and without the addition of n-HA and MCC. The results show that the material properties are related to the processing conditions and chemical composition of the blends. While the addition of n-HA and MCC generally improves crystallinity and elongation, meeting the standards set by EN 17033 for agricultural applications presents significant challenges.

Mechanical testing showed that although we could achieve high elongation, the critical factor of strain did not comply with the requirements of EN 17033. This drawback is particularly evident in agricultural applications, where materials must withstand dynamic environmental stresses. Here, flexibility and scalability are as important as strength. Our data indicate that while increasing MCC content can enhance ductility and water absorption to some extent, there is a threshold, as shown by the decrease in performance of Sample 18 water absorption rate. The PLA-majority samples (Sample 15 to 18) also showed very

good UV resistance, indicating that the PLA/PBAT blend can safely spend the growth cycle of crops outdoors.

In summary, our study demonstrates that the composition and processing of PBAT/PLA blends require a delicate balance to meet the stringent requirements of agricultural applications. Optimizing these materials has clear potential, but further research is needed to refine their properties. Our goal is to create mixtures that not only meet established standards but also perform exceptionally well under real-world conditions encountered in the agricultural sector.

Going forward, optimization of blend compositions, long-term environmental impact studies, evaluation of new additives and antibiotic adsorption deserve further research to realize the full potential of PLA/PBAT blends in agricultural applications. Continued research should focus on fine-tuning the ratio of PLA to PBAT and the concentration of additives to improve the mechanical strength and flexibility of the blends and ensure compliance with industry standards. It is crucial to conduct long-term field studies to assess the environmental impact of these biodegradable films, particularly their degradation behavior and interaction with soil microbiota. Investigate whether the addition of n-HA and MCC can discover new blends with superior properties. Finally given concerns about antibiotic resistance genes, it is crucial to study the antibiotic adsorption

capacity of these films, especially in situations where they may come into contact with treated wastewater.

By addressing these future research directions, this work aims to make a significant contribution to the development of sustainable agricultural practices, reduce the environmental footprint of plastic use in agriculture, and move towards a greener future.

APPENDIX A

DETAIL DATA OF TENSILE TEST

Tensile test results are provided detailly in the following Tables.

Table A.1 Tensile stress (MPa) and strain (%) at break for each sample

Name	stress 1	stress 2	stress 3	strain 1	strain 2	strain 3
100PL A	55.88	60.49	52.39	4.15	4.44	3.89
100PL A*	45.82	48.03	47.24	2.01	2.45	2.52
100PB AT (0.48 mm)				1000	1000	1000
100PB AT (0.13 mm)	24.29	23.11		387.7	348.5	
PE	15.39	21.28	13.79	1000	1000	1000
70/30	7.61	7.4545 45	8.0333 33	16.31	13.18	21.06
80/20	7.52	7.29	7.69	72.45	47.06	74.85
90//10	9.68	9.48	9.8471 71	359.20	480.47	442.69
90//10	8.54	7.87	7.62	282.71	352.21	276.44
70/30 *	7.97	7.0777 67	7.71	23.19	10.93	11.70
80/20 *	8.9710 57	7.4361 05	8.99	194.61	172.21	207.78
90/10 *	8.2413 91	8.6469 65	8.1689 61	255.60 04	219.79 56	213.93 12

2HA	60.42	52.55	59.67	1.11	1.13	1.16
4HA	65.75	45.32	40.74	1.25	1.10	1.22
6HA	51.07	45.59	49.84	1.75	1.75	1.22
4MCC	44.17	46.39	43.19	1.37	1.32	1.11
6MCC	37.73	41.41	38.05	3.72	3.49	3.49
7MCC	40.74	35.78	36.12	4.79	4.90	4.67

REFERENCES

- Abed, H. Y., Hameed, N. J., & Salim, E. T. (2023). Influence of nano-hydroxyapatite particles on the mechanical and antibacterial properties of polycarbonate films. *Materials Research Express*, *10*(8), 085301. <https://doi.org/10.1088/2053-1591/acec35>
- Albert, A., Seidlitz, H. K., & Winkler, J. B. (2005). solar simulators as a tool for assessing the impact of UV radiation on organisms and ecosystems. ResearchGate. Retrieved from https://www.researchgate.net/publication/230734344_solar_simulators_as_a_tool_for_assessing_the_impact_of_UV_radiation_on_organisms_and_ecosystems
- Amare, G., & Desta, B. (2021). Coloured plastic mulches: impact on soil properties and crop productivity. *Chemical and Biological Technologies in Agriculture*, *8*(1). <https://doi.org/10.1186/s40538-020-00201-8>
- Arias-Andrés, M., Klümper, U., Rojas-Jiménez, K., & Grossart, H. (2018). Microplastic pollution increases gene exchange in aquatic ecosystems. *Environmental Pollution*, *237*, 253–261. <https://doi.org/10.1016/j.envpol.2018.02.058>
- Bandopadhyay, S., Martín-Closas, L., Pelacho, A. M., & DeBruyn, J. M. (2018). Biodegradable plastic mulch films: Impacts on soil microbial communities and ecosystem functions. *Frontiers in Microbiology*, *9*. <https://doi.org/10.3389/fmicb.2018.00819>
- Bandyopadhyay, K., Acharya, C., & Hati, K. M. (2023). Mulches and cover crops part I: Types. In *Elsevier eBooks* (pp. 392–400). <https://doi.org/10.1016/b978-0-12-822974-3.00199-3>
- Baskar, K., Anusuya, T., & Venkatasubbu, G. D. (2017). Mechanistic investigation on microbial toxicity of nano hydroxyapatite on implant associated pathogens. *Materials Science and Engineering: C*, *73*, 8–14. <https://doi.org/10.1016/j.msec.2016.12.060>
- Brunton, P., Davies, R. P. W., Burke, J., Smith, A. B., Aggeli, A., Brookes, S. J., & Kirkham, J. (2013). Treatment of early caries lesions using biomimetic self-assembling peptides – a clinical safety trial. *British Dental Journal*, *215*(4), E6. <https://doi.org/10.1038/sj.bdj.2013.741>
- Deng, B., Li, W., Lü, H., & Zhu, L. (2022). Film mulching reduces antibiotic resistance genes in the phyllosphere of lettuce. *Journal of*

Environmental Sciences-china, 112, 121–128.
<https://doi.org/10.1016/j.jes.2021.04.032>

- Fu, Y., Wu, G., Bian, X., Zeng, J., & Weng, Y. (2020). Biodegradation Behavior of Poly(Butylene Adipate-Co-Terephthalate) (PBAT), Poly(Lactic Acid) (PLA), and Their Blend in Freshwater with Sediment. *Molecules*, 25(17), 3946.
<https://doi.org/10.3390/molecules25173946>
- Gao, X., Xie, D., & Yang, C. (2021). Effects of a PLA/PBAT biodegradable film mulch as a replacement of polyethylene film and their residues on crop and soil environment. *Agricultural Water Management*, 255, 107053. <https://doi.org/10.1016/j.agwat.2021.107053>
- Gewert, B., Plassmann, M., Sandblom, O., & MacLeod, M. (2018). Identification of Chain Scission Products Released to Water by Plastic Exposed to Ultraviolet Light. *Environmental Science & Technology Letters*, 5(5), 272–276.
<https://doi.org/10.1021/acs.estlett.8b00119>
- Griffin, M., Premakumar, Y., Seifalian, A., Butler, P. E., & Szarko, M. (2016). Biomechanical Characterization of Human Soft Tissues Using Indentation and Tensile Testing. *Journal of Visualized Experiments*, (118). <https://doi.org/10.3791/54872>
- Jeya, S., & Sundaresan, B. (2023). Influence of Strontium titanate on the ionic conductivity of sodium ion-based polymer electrolyte. *Solid State Ionics*, 399, 116301. <https://doi.org/10.1016/j.ssi.2023.116301>
- Jia, X., Shi, N., Tang, W., Su, Z., Chen, H., Tang, Y., . . . Zhao, L. (2022a). Nano-hydroxyapatite increased soil quality and boosted beneficial soil microbes. *Plant Nano Biology*, 1, 100002.
<https://doi.org/10.1016/j.plana.2022.100002>
- Jian, J., Xiangbin, Z., & Xianbo, H. (2020). An overview on synthesis, properties and applications of poly(butylene-adipate-co-terephthalate)–PBAT. *Advanced Industrial and Engineering Polymer Research*, 3(1), 19–26. <https://doi.org/10.1016/j.aiepr.2020.01.001>
- Jiao, J., Zeng, X., & Xianbo, H. (2020). An overview on synthesis, properties and applications of poly(butylene-adipate-co-terephthalate)–PBAT. *Advanced Industrial and Engineering Polymer Research*, 3(1), 19–26. <https://doi.org/10.1016/j.aiepr.2020.01.001>
- Kumar, M., Xiong, X., He, M., Tsang, D. C., Gupta, J., Khan, E., . . . Bolan, N. (2020). Microplastics as pollutants in agricultural soils. *Environmental Pollution*, 265, 114980.
<https://doi.org/10.1016/j.envpol.2020.114980>
- Lay, M., Thajudin, N. L. N., Hamid, Z. a. A., Rusli, A., Abdullah, M. A., & Shuib, R. K. (2019). Comparison of physical and mechanical properties of PLA, ABS and nylon 6 fabricated using fused deposition

- modeling and injection molding. *Composites Part B: Engineering*, 176, 107341. <https://doi.org/10.1016/j.compositesb.2019.107341>
- Lee, Y., Cho, J., Sohn, J., & Kim, H. (2023). Health effects of microplastic exposures: current issues and perspectives in South Korea. *Yonsei Medical Journal*, 64(5), 301. <https://doi.org/10.3349/ymj.2023.0048>
- Leow, A. T. C., Leow, A. T. C., & Rahman, R. N. Z. R. A. (2021). MICROBIAL DEGRADATION OF POLYLACTIC ACID BIOPLASTIC. *Journal of Sustainability Science and Management*, 16(7), 299–317. <https://doi.org/10.46754/jssm.2021.10.021>
- Li, J., Zhang, K., & Zhang, H. (2018). Adsorption of antibiotics on microplastics. *Environmental Pollution*, 237, 460–467. <https://doi.org/10.1016/j.envpol.2018.02.050>
- Li, X., Zheng, G., Li, Z., & Fu, P. (2024). Formulation, performance and environmental/agricultural benefit analysis of biomass-based biodegradable mulch films: A review. *European Polymer Journal*, 203, 112663. <https://doi.org/10.1016/j.eurpolymj.2023.112663>
- Li, Y., Tao, L., Wang, Q., Wang, F., Li, G., & Song, M. (2023). Potential Health impact of Microplastics: A review of environmental distribution, human exposure, and toxic effects. *Environment & Health*, 1(4), 249–257. <https://doi.org/10.1021/envhealth.3c00052>
- Liu, H., & Zhang, J. (2011). Research progress in toughening modification of poly(lactic acid). *Polymer Physics*, 49(15), 1051–1083. <https://doi.org/10.1002/polb.22283>
- Liu, W., Fei, M., Ban, Y., Jia, A., & Qiu, R. (2017a). Preparation and Evaluation of Green Composites from Microcrystalline Cellulose and a Soybean-Oil Derivative. *Polymers*, 9(12), 541. <https://doi.org/10.3390/polym9100541>
- Ludwiczak, J., Dmitruk, A., Skwarski, M., Kaczyński, P., & Makuła, P. (2023). UV resistance and biodegradation of PLA-based polymeric blends doped with PBS, PBAT, TPS. *International Journal of Polymer Analysis and Characterization*, 28(4), 366–382. <https://doi.org/10.1080/1023666x.2023.2218696>
- Lyu, J. S., & Han, J. (2023). Scale-up fabrication of a biodegradable PBAT/PLA composite film compatibilized with a chain extender for industrial agricultural mulch film application. *Composites Part C: Open Access*, 12, 100397. <https://doi.org/10.1016/j.jcomc.2023.100397>
- Mahapatro, A., & Singh, D. K. (2011). Biodegradable nanoparticles are excellent vehicle for site directed in-vivo delivery of drugs and vaccines. *Journal of Nanobiotechnology*, 9(1), 55. <https://doi.org/10.1186/1477-3155-9-55>

- Michaelis, C., & Grohmann, E. (2023). Horizontal gene transfer of antibiotic resistance genes in biofilms. *Antibiotics*, *12*(2), 328. <https://doi.org/10.3390/antibiotics12020328>
- Murariu, M., & Dubois, P. (2016). PLA composites: From production to properties. *Advanced Drug Delivery Reviews*, *107*, 17–46. <https://doi.org/10.1016/j.addr.2016.04.003>
- Musioł, M., Sikorska, W., Janeczek, H., Wałach, W., Hercog, A., Johnston, B., & Rydz, J. (2018). (Bio)degradable polymeric materials for a sustainable future – part 1. Organic recycling of PLA/PBAT blends in the form of prototype packages with long shelf-life. *Waste Management*, *77*, 447–454. <https://doi.org/10.1016/j.wasman.2018.04.030>
- Naseri, N., Deepa, B., Mathew, A. P., Oksman, K., & Girandon, L. (2016). Nanocellulose-Based Interpenetrating Polymer Network (IPN) hydrogels for cartilage applications. *Biomacromolecules*, *17*(11), 3714–3723. <https://doi.org/10.1021/acs.biomac.6b01243>
- Nofar, M., Heuzey, M. C., Carreau, P. J., Kamal, M. R., & Randall, J. (2016). Coalescence in PLA-PBAT blends under shear flow: Effects of blend preparation and PLA molecular weight. *Journal of Rheology*, *60*(4), 637–648. <https://doi.org/10.1122/1.4953446>
- Nofar, M., Maani, A., Sojoudi, H., Heuzey, M. C., & Carreau, P. J. (2015). Interfacial and rheological properties of PLA/PBAT and PLA/PBSA blends and their morphological stability under shear flow. *Journal of Rheology*, *59*(2), 317–333. <https://doi.org/10.1122/1.4905714>
- Rahman, M. M., Islam, M. S., & Li, G. S. (2018). Development of PLA/CS/ZnO nanocomposites and optimization its mechanical, thermal and water absorption properties. *Polymer Testing*, *68*, 302–308. <https://doi.org/10.1016/j.polymertesting.2018.04.026>
- Saxena, V., Hasan, A., & Pandey, L. M. (2017). Effect of Zn/ZnO integration with hydroxyapatite: a review. *Materials Technology*, *33*(2), 79–92. <https://doi.org/10.1080/10667857.2017.1377972>
- SCIMED. (2021, November 2). What is X-Ray Diffraction (XRD). Retrieved from <https://www.scimed.co.uk/education/what-is-x-ray-diffraction-xrd/>
- Seyoum, M. M., Lichtenberg, R., Orlofsky, E., Bernstein, N., & Gillor, O. (2022). Antibiotic resistance in soil and tomato crop irrigated with freshwater and two types of treated wastewater. *Environmental Research*, *211*, 113021. <https://doi.org/10.1016/j.envres.2022.113021>
- Seyoum, M. M., Obayomi, O., Bernstein, N., Williams, C. F., & Gillor, O. (2022). The dissemination of antibiotics and their corresponding resistance genes in treated effluent-soil-crops continuum, and the

- effect of barriers. *Science of the Total Environment*, 807, 151525.
<https://doi.org/10.1016/j.scitotenv.2021.151525>
- Sintim, H. Y., & Flury, M. (2017). Is Biodegradable Plastic Mulch the Solution to Agriculture's Plastic Problem? *Environmental Science & Technology*, 51(3), 1068–1069.
<https://doi.org/10.1021/acs.est.6b06042>
- Ślęzak, R., Krzystek, L., Puchalski, M., Krucińska, I., & Sitarski, A. (2023). Degradation of bio-based film plastics in soil under natural conditions. *Science of the Total Environment*, 866, 161401.
<https://doi.org/10.1016/j.scitotenv.2023.161401>
- Sopyan, I., Mel, M., Ramesh, S., & Khalid, K. A. (2007). Porous hydroxyapatite for artificial bone applications. *Science and Technology of Advanced Materials*, 8(1–2), 116–123.
<https://doi.org/10.1016/j.stam.2006.11.017>
- Sritham, E., Phunsombat, P., & Chaishome, J. (2018). Tensile properties of PLA/PBAT blends and PLA fibre-reinforced PBAT composite. *MATEC Web of Conferences*, 192, 03014.
<https://doi.org/10.1051/mateconf/201819203014>
- Subrahmaniyan, K., & Ngouajio, M. (2012). Polyethylene and biodegradable mulches for agricultural applications: a review. *Agronomy for Sustainable Development*, 32(2), 501–529.
<https://doi.org/10.1007/s13593-011-0068-3>
- Tsou, C., Chen, Z., Yuan, S., Ma, Z., Wu, C., Yang, T., . . . De Guzman, M. R. (2022). The preparation and performance of poly(butylene adipate) terephthalate/corn stalk composites. *Current Research in Green and Sustainable Chemistry*, 5, 100329.
<https://doi.org/10.1016/j.crgsc.2022.100329>
- Weng, Y., Jin, Y., Meng, Q., Wang, L., Zhang, M., & Wang, Y. (2013). Biodegradation behavior of poly(butylene adipate-co-terephthalate) (PBAT), poly(lactic acid) (PLA), and their blend under soil conditions. *Polymer Testing*, 32(5), 918–926.
<https://doi.org/10.1016/j.polymertesting.2013.05.001>
- Witt, U., Einig, T., Yamamoto, M., Kleeberg, I., Deckwer, W., & Müller, R. (2001). Biodegradation of aliphatic–aromatic copolyesters: evaluation of the final biodegradability and ecotoxicological impact of degradation intermediates. *Chemosphere*, 44(2), 289–299.
[https://doi.org/10.1016/s0045-6535\(00\)00162-4](https://doi.org/10.1016/s0045-6535(00)00162-4)
- Xiang, S., Feng, L., Bian, X., Gao, L., & Chen, X. (2020). Evaluation of PLA content in PLA/PBAT blends using TGA. *Polymer Testing*, 81, 106211. <https://doi.org/10.1016/j.polymertesting.2019.106211>
- Yan, D., Wang, Z., Guo, Z., Ma, Y., Wang, C., Tan, H., & Zhang, Y. (2020). Study on the properties of PLA/PBAT composite modified by

- nanohydroxyapatite. *Journal of Materials Research and Technology*, 9(5), 11895–11904. <https://doi.org/10.1016/j.jmrt.2020.08.062>
- Yang, L., & Lü, L. (2013). The influence of sample thickness on the tensile properties of pure Cu with different grain sizes. *Scripta Materialia*, 69(3), 242–245. <https://doi.org/10.1016/j.scriptamat.2013.04.009>
- Yin, M., Li, Y., Fang, H., & Chen, P. (2019). Biodegradable mulching film with an optimum degradation rate improves soil environment and enhances maize growth. *Agricultural Water Management*, 216, 127–137. <https://doi.org/10.1016/j.agwat.2019.02.004>
- Zhang, M., Jia, H., Weng, Y., & Li, C. (2019). Biodegradable PLA/PBAT mulch on microbial community structure in different soils. *International Biodeterioration & Biodegradation*, 145, 104817. <https://doi.org/10.1016/j.ibiod.2019.104817>
- Zhang, S., Li, L., & Kumar, A. (2008). *Materials Characterization Techniques* (1st ed.). CRC Press.
- Zhang, W., & Xu, Y. (2019). Experimental Studies of Mechanical Properties of Polycarbonate. *Mechanical Properties of Polycarbonate*, 1–28. <https://doi.org/10.1016/b978-1-78548-313-4.50001-7>
- Zhang, Y., Lu, J., Wu, J., Wang, J., & Luo, Y. (2020). Potential risks of microplastics combined with superbugs: Enrichment of antibiotic resistant bacteria on the surface of microplastics in mariculture system. *Ecotoxicology and Environmental Safety*, 187, 109852. <https://doi.org/10.1016/j.ecoenv.2019.109852>
- Zhang, Y., Zheng, X., Xu, X., Cao, L., Zhang, H., Zhang, H., . . . Cao, X. (2022). Straw return promoted the simultaneous elimination of sulfamethoxazole and related antibiotic resistance genes in the paddy soil. *Science of the Total Environment*, 806, 150525. <https://doi.org/10.1016/j.scitotenv.2021.150525>
- Zheng, W., Zhang, Z., Li, R., & Lei, Z. (2018a). Removal of veterinary antibiotics from anaerobically digested swine wastewater using an intermittently aerated sequencing batch reactor. *Journal of Environmental Sciences-china*, 65, 8–17. <https://doi.org/10.1016/j.jes.2017.04.011>
- Zhou, Q., Zhang, J., Zhang, M., Wang, X., Zhang, D., & Pan, X. (2022). Persistent versus transient, and conventional plastic versus biodegradable plastic? —Two key questions about microplastic-water exchange of antibiotic resistance genes. *Water Research*, 222, 118899. <https://doi.org/10.1016/j.watres.2022.118899>